

M. THESIS

8

FINITE ELEMENT SOLUTION  
OF TEMPERATURE TRANSIENTS  
IN POWER CABLES

A MASTER THESIS  
SUBMITTED TO THE DEPARTMENT OF ELECTRICAL ENGINEERING  
AND THE COMMITTEE ON THE FACULTY OF ENGINEERING  
OF MIDDLE EAST TECHNICAL UNIVERSITY GAZIANTEP CAMPUS  
IN PARTIAL FULFILLMENT OF THE REQUIREMENTS  
FOR THE DEGREE OF  
MASTER OF SCIENCE

By  
Doğan Anakök  
February 1982

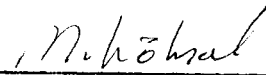
I certify that I have read this thesis and that in my opinion it is fully adequate, in scope and quality, as a thesis for the degree of Master of Science.



Supervisor

Assoc.Prof.Dr. Arif Ertas

I certify that this thesis satisfies all the requirements as a thesis for the degree of Master of Science.



Chairman of the Department

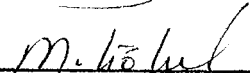
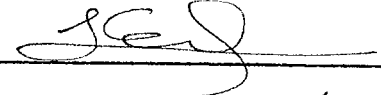
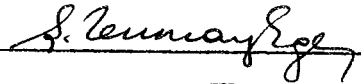
Examining Committee in Charge :

. . Doç.Dr. Arif Ertas . . . . .

. . Y.Doç.Dr. Tuncay Ege . . . . .

. . Y.Doç.Dr. Halit Eren . . . . .

. . Y.Doç.Dr. Muhammed Köksal . . . . .



Committee Chairman

ABSTRACT  
FINITE ELEMENT SOLUTION  
OF TEMPERATURE TRANSIENTS  
IN POWER CABLES

ANAKÖK, Doğan  
M.Sc. in E.E  
Supervisor: Assoc.Prof.Dr.Arif Ertas  
February, 1982

A general finite element program is developed to solve thermal transient problems related with the buried power cables whose thermal transient behaviour is governed by a general second order partial differential equation. The formulation is based on variational principles and for this purpose the solution domain is divided into a finite numbers of triangular elements and the associated functional is formed. A set of algebraic equations are obtained after minimizing the functionals corresponding to the governing field equation. Using another numerical procedure for the transient part of these algebraic equations, the nodal temperatures are obtained in the transient period. The integrations appearing in the functionals are performed by the aid of area coordinates.

The method is applied both to single and three phase cables in finding their thermal transient behaviour.

Key words : Thermal field, Finite element

## ÖZET

### GÜÇ KABLOLARINDA GEÇİCİ SICAKLIKLARIN SONLU ELEMEN TEKNIĞI İLE ÇÖZÜMÜ

ANAKÖK, Doğan  
Yüksek Lisans Tezi: Elek. Müh. Bölümü  
Tez Yöneticisi: Doç.Dr. Arif Ertuş  
Şubat, 1982

Geçici ısı davranışı genel bir ikinci derece kısmi türev denklemine göre değişen toprağa gömülü güç kablolarının ısı geçici rejimlerini çözümleyen genel bir sonlu eleman programı geliştirildi. Çözümleme değişim prensibine dayanmakta ve bu amaçla çözüm bölgesi belirli sayıda üçgen elemanlara bölünmekte ve ilgili işlevsel oluşturulmaktadır. Alan denklemine karşılık gelen işlevsellerin en küçükleştirilmesi ile bir dizi cebirsel denklem elde edilmektedir. Bu denklemlerin geçici rejim kısmı ile ilgili olarak geliştirilen diğer bir sayısal yöntem ile, geçici rejim dönemindeki düğüm sıcaklıkları elde edilmektedir. İşlevsellerde yer alan tümler işlemleri alan koordinatları yardımı ile yapılmaktadır.

Bu yöntem tek ve üç fazlı yer altı kablolarının geçici rejim ısı davranışlarının bulunmasında kullanılmaktadır.

Anahtar sözcükler : Isıl alan, sonlu eleman

## ACKNOWLEDGEMENT

I express my gratitude and sincere thanks to Assoc. Prof. Dr. Arif Ertaş for his patient supervision, persistent help and encouragement in this effort.

I also like to thank to my sister Mrs. Tülin Karakaya for her carefull typing.

## CONTENTS

	<u>Page</u>
LIST OF SYMBOLS	viii
CHAPTER I	1
INTRODUCTION	1
CHAPTER II	
METHOD OF FINITE ELEMENTS	
2.1    Heat conduction problems	3
2.1.1    Heat conduction in power cables	5
2.1.2    Boundary conditions	7
2.2    Variational finite element method	8
2.2.1    Shape functions	11
2.2.2    Area coordinates	12
2.2.3    Application of finite element method to thermal transient problems	15
2.2.3.1    Energy minimisation of one element	16
2.2.3.2    Assembly of elements	19
2.2.3.3    Mathematical consideration of Boundary conditions in the solution of time dependent problem.	22
CHAPTER III	
SOME PRACTICAL ASPECTS OF FINITE ELEMENT METHOD AND PROGRAM DEVELOPMENT	
3.1    Modelling of a problem	26
3.1.1    Node numbering and bandwidth	30
3.1.2    Automatic mesh generation	32
3.2    Solution of simultaneous equations	36
3.2.1    Gaussian elimination using a full matrix	36
3.2.2    Gaussian elimination for a banded matrix	37
3.2.3    Square root method	38
3.3    Convergence of finite element methods	40
3.4    Truncation error	42
3.5    The program	44

CHAPTER IV  
APPLICATIONS

4.1	Introduction	48
4.2	Simple cable problem	50
4.2.1	Analytical solution	51
4.2.2	Finite element solution	51
4.3	Heat analysis of a 35KV, 95 mm <sup>2</sup> cable	57
4.3.1	Modelling of the problem	57
4.3.2	Program and the discussion of the results	61
4.4	Heat analysis of a three phase 275KV cable	71
4.4.1	Modelling	72
4.4.2	Results and Discussions	75

CHAPTER V  
CONCLUSIONS

5.1	Concluding remarks on finite element approach	79
5.2	Temperature transients in power cables	81
5.3	Future work	82

APPENDIX

A.	VARIATIONAL FORMULATION	83
B.	HIGHER ORDER SHAPE FUNCTIONS	87
C.	EXACT SOLUTION OF STEADY STATE TEMPERATURE DISTRIBUTION IN INSULATED ELECTRIC CABLE	88

REFERENCES	90
------------	----

## LIST OF SYMBOLS

A	: Area
C	: Heat capacity coefficient
D	: Product of J and V
$E_T$	: Truncation error
H	: Heat conductivity matrix
I	: Current
J	: Jocabian matrix
L	: Lower triangular matrix
N	: Shape function
P	: Heat capacity matrix
Q	: Heat flux
R	: Resistance
S	: Surface
$T^e$	: Temperature of element
T	: Temperature
$T_a$	: Air temperature
U	: Upper triangular matrix
V	: Volume
$V_g$	: Potential
a	: Coaxial cable inner radius
b	: Coaxial cable outer radius
c	: Specific heat
d	: Distance
f	: Frequency
$h^e$	: Heat conductivity matrix for each element
k	: Thermal conductivity



$n$	: integer
$p$	: Resistivity
$q$	: Internal heat generation
$r$	: Radius
$s$	: Surface element
$t$	: time
$\rho$	: Density
$\theta$	: Resistance temperature coefficient
$\epsilon$	: Dielectric constant
$\alpha$	: Heat transfer coefficient
$\chi$	: Energy functional
$\omega_i, \omega_j, \omega_m$	: Area coordinates
$\Delta$	: Incremental value
$\phi$	: Angle in polar coordinates
$\tan\delta$	: Loss angle
HBW	: Half-bandwidth

CHAPTER I  
INTRODUCTION

The story of the finite element method in engineering begins back in the early 1950's. Attempts were then being made to apply the matrix methods that were successful with discrete structures to continuous structures by subdividing the structure into a finite number of hypothetical elements. In 1956 the group formed by Turner at the Boeing Aircraft Company described a procedure of this type using several features of the finite element method(1). Following this we observe the rapid development on the application of the finite element method in a wide range of problems of structural engineering and solid mechanics. In the early days the method is particularly based on stiffness or so called equilibrium procedures.

In recent years the finite element method has been applied widely to non-structural problems, and the formulation is now mainly based on variational principles or weighted residual procedures. A detailed presentation is given in a text by Zienkiewicz(?).

Some of the areas in which the finite element method has been applied are; aircraft, automotive, building structures, electromagnetic fields, heat transfer, statistics etc.

A study as a M.Sc. thesis is made in METU(3) for the solution of the electrical field variation in and around of several insulators used for some h.v. switchgear and also determining the electrical and thermal field distribution in a coaxial cable.

This work applies the finite element method to the solution of thermal transient problems. A general finite element program is developed to solve thermal transient problems related with the buried power cables whose thermal transient behaviour is governed by the second order partial differential equation,  $\text{div}(k \text{ grad } T) + q - C \frac{\partial T}{\partial t} = 0$ .

The steps in developing the finite element program are outlined generally as follows,

- (i) The physical region of the problem is subdivided into subregions or finite elements.
- (ii) Dependent variables are approximated in functional form over each element and hence over the whole domain. The parameters of this approximation as a result become the unknowns of the problem.
- (iii) Substitution of the approximations into the governing parabolic equation yields a set of simultaneous algebraic equations considering also the relevant boundary conditions.
- (iv) Considering the variation of the unknown is linear within each time interval, step by step solution of these equations yields the approximate solution to the time dependent problem with the prescribed initial conditions.

CHAPTER II  
METHOD OF FINITE ELEMENTS

2.1 Heat conduction problems

The partial differential equation of heat conduction in solid bodies is derived by considering the energy balance on a differential element of volume ( $dx dy dz$ ) of a material subject to a conduction process and shown in Fig.2.1.

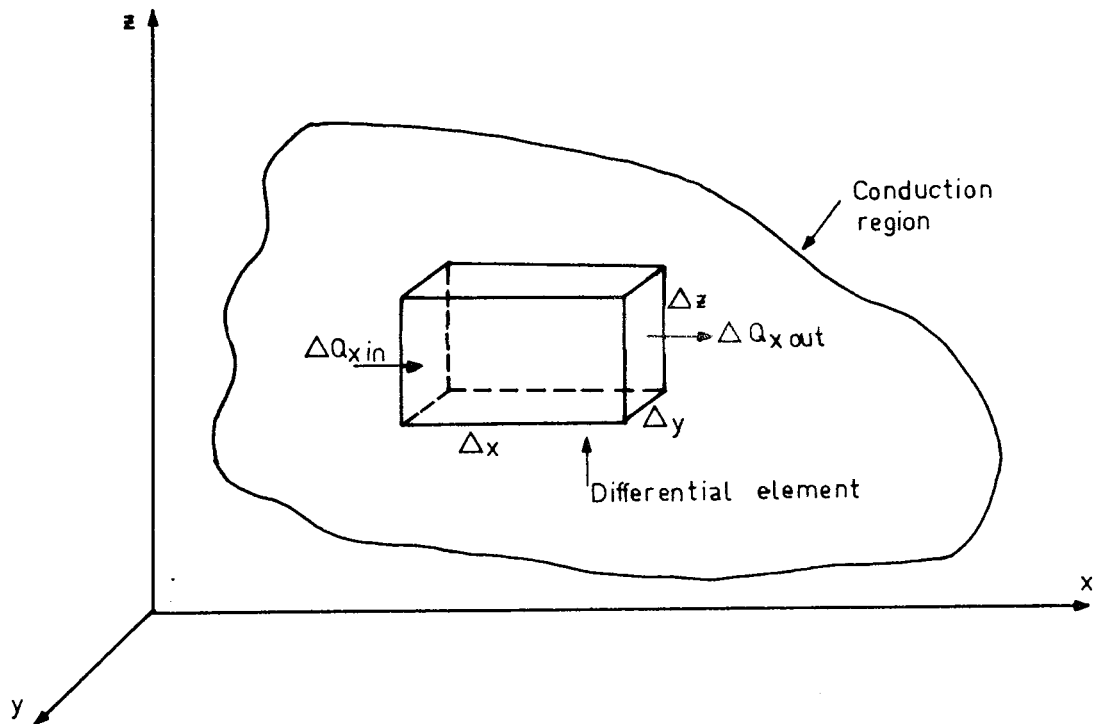


FIGURE 2.1 Differential element in thermal conduction analysis.

The net energy gain in time  $\Delta t$  across the six faces by conduction is added to the energy generation in time  $\Delta t$  and the sum is set equal to the change in time  $\Delta t$  of energy stored in the mass inside the volume element.

Basic Fourier Law of heat conduction reveals that the rate at which heat is flowing across a given section is proportional to the temperature gradient measured normal to that section(4). Thus for thermal fields, the rate of heat flow  $Q$  across unit

area is related to the temperature gradient  $\bar{U}$  by,

$$\bar{Q} = k\bar{U} \quad (2.1)$$

where,

$$\bar{U} = -\text{grad } T \quad (2.2)$$

and,  $T$  is temperature, and  $k$  is the coefficient of thermal conductivity of the solid. The negative sign in equation(2.2) is required to make the equation consistent, i.e that heat will flow into a region of lower temperature, giving a positive value for  $Q$  when temperature gradient is negative. Now, any volume  $V$ , bounded by a closed surface  $S$ , gains heat by conduction at a rate of,

$$- \int_S \bar{Q} \cdot \bar{n} ds \quad (2.3)$$

where  $\bar{n}$  is the unit vector normal to  $ds$ . This causes increase of heat inside the solid by the rate of

$$\int_V c\rho \frac{\partial T}{\partial t} dV \quad (2.4)$$

such that,

$$- \int_S \bar{Q} \cdot \bar{n} ds = \int_V c\rho \frac{\partial T}{\partial t} dV \quad (2.5)$$

using the divergence theorem,  $\int_V c\rho \frac{\partial T}{\partial t} dV = -\int_V \text{div}\bar{Q}dV$  ,

$$\text{div}\bar{Q} = - c\rho \frac{\partial T}{\partial t} \quad (2.7)$$

using equations (2.1), (2.2) and (2.7),  $\text{div} (k \text{ grad } T) = c\rho \frac{\partial T}{\partial t}$

If  $k$  is a constant, Equation (2.8) reduces to,

$$k \text{ div} (\text{grad } T) = c\rho \frac{\partial T}{\partial t} \quad (2.9)$$

If there is heat generation in the volume,

$$k \text{ div} (\text{grad } T) + q = c\rho \frac{\partial T}{\partial t} \quad (2.10)$$

where,

$t$  : time (sec)

$k$  : thermal conductivity ( $\text{cal.cm}^{-1} \cdot \text{sec}^{-1} \cdot ^\circ\text{C}^{-1}$ )

$T$  : temperature ( $^\circ\text{C}$ )

$c$  : specific heat of the material ( $\text{cal. gr}^{-1} \cdot ^\circ\text{C}^{-1}$ )

$\rho$  : density of material ( $\text{gr.cm}^{-3}$ )

$q$  : Internal heat generation ( $\text{cal. sec}^{-1} \cdot \text{cm}^{-3}$ )  
 $C=\rho c$  : heat capacity coefficient ( $\text{cal. cm}^{-3} \cdot ^\circ\text{C}^{-1}$ )

### 2.1.1 Heat conduction in power cables

A transient thermal field analysis is applied to underground power cables using equation (2.10) which is a parabolic partial differential equation. An underground cable is mainly composed of a cable core (conductor), main insulation, sheath and sheath insulation as seen in Fig.2.2.

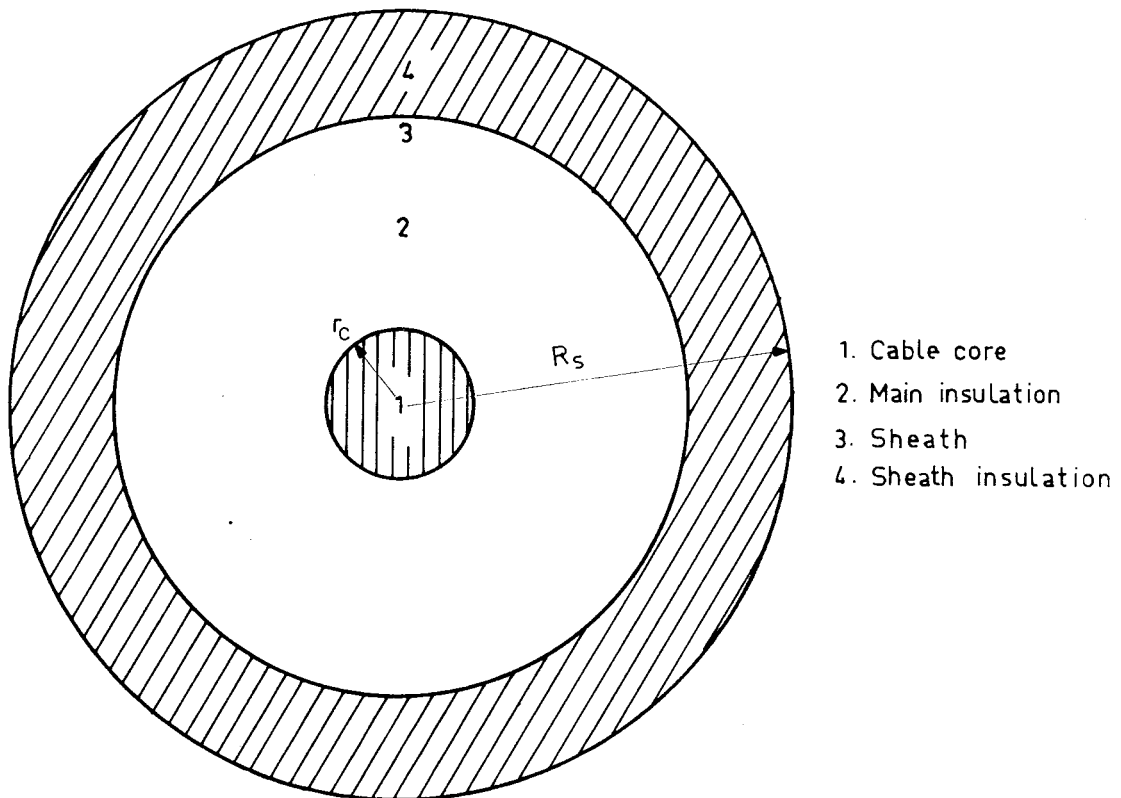


FIGURE 2.2 A typical power cable.

Heat generation in a single cable is mainly caused by the heat dissipation in the power core, dielectric losses through the insulation, and sheath losses.

Due to the resistance of the conductor, heat energy is produced within the conductor by the current passing through it, which is equal to,

$$I^2 R \text{ (Watts.cm}^{-1}\text{)} \quad (2.11)$$

where 1 watt = 0.238846 cal.sec<sup>-1</sup>

I : current through the conductor (amper)

R : resistance of the conductor (ohm.cm<sup>-1</sup>)

The resistance of any copper conductor of known resistivity can be found as,

$$R = \rho \left[ 1 + \theta(T - T_a) \right] / \pi r_c^2 \quad (2.12)$$

where

$\rho$  : resistivity of the conductor (ohm.mm<sup>2</sup>.m<sup>-1</sup>)

$\theta$  : resistance temperature coefficient of the conductor at temperature T (°C<sup>-1</sup>)

$T_a$  : temperature of the conductor (°C)

On the other hand internal heat generation in the main insulation is mainly affected by the electric field intensity and temperature of the dielectric insulation. Therefore for any particular finite element,

$$q_e = f(E_e, T_e) \quad (2.13)$$

Taking dielectric permittivity constant, the internal heat generation is given by(5,6);

$$q = 2\pi f \epsilon_0 \epsilon_r \tan \delta (T) |\text{grad } V|^2 \text{ (cal.sec}^{-1}\text{.cm}^{-3}\text{)} \quad (2.14)$$

where,

f : frequency (Hz)

$\epsilon_r$  : relative permittivity

$\epsilon_0$  : permittivity of free space ( 0.885x10<sup>-12</sup> farads. m<sup>-1</sup>)

V : applied voltage

and where  $2\pi f \epsilon_0 \epsilon_r \tan \delta (T)$  is the a.c conductivity of the dielectric and  $\tan \delta (T)$  is the loss angle being a function of temperature. In this work electric field is assumed to be evenly distributed over all elements of the dielectric region. The second and third assumptions are made considering both conductor resistance and loss angle being temperature independent.

Another heat source in power cables are shield losses which are taken into account as constant heat fluxes at the shield

are taken into account as constant heat fluxes at the shield boundary. Especially at short circuit conditions some amount of current passing through the shield causes a dissipation due to the shield resistance. Consequently a heat flux flows from the shield surface towards the surrounding and is determined by;

$$k \text{ grad } T = Q_s = \frac{I^2 R_s}{2\pi r_s} \quad \text{watts/cm}^2 \quad (2.15)$$

Where  $R_s$  is the shield resistance and  $r_s$  is the radius of the shield. The consideration given to heat fluxes as a kind of boundary condition is represented in subsequent chapters.

### 2.1.2 Boundary conditions

The most common boundary conditions which are encountered in a heat conduction problem of power cables are;

- (i) the temperature  $T$  is specified at the boundary,
- (ii) the normal gradient  $\frac{\partial T}{\partial n}$  is zero at the boundary,
- (iii) the heat flux  $Q$  per unit area at the boundary surface is constant,
- (iv) the convection loss at the boundary is equal to  $\alpha(T - T_a)$  where  $T_a$  is the ambient temperature and  $\alpha$  is the heat transfer coefficient.

When there is a constant heat flux per unit area of the boundary surface or a convection loss at the boundary, the energy functional will take the form,

$$\chi = \iint \left\{ \frac{1}{2} k \left[ \left( \frac{\partial T}{\partial x} \right)^2 + \left( \frac{\partial T}{\partial y} \right)^2 \right] - (q - c \frac{\partial T}{\partial t}) T \right\} dx dy - \int_c Q T ds + \int_c \alpha \left( \frac{1}{2} T^2 - T_a T \right) ds$$

When both  $Q$  and  $\alpha$  are zero, the boundary is assumed to be non-conducting, which means that the normal gradient  $\frac{\partial T}{\partial n}$  is zero.

Therefore typical boundary conditions which will be dealt in this study are Dirichlet, Neumann and mixed types respectively. At each part of the boundary, one of these must be specified.



## 2.2 The variational finite element method

As mentioned previously, the first step in adopting finite element method is to divide the continuum into two or three dimensional finite elements, which are separated by straight or curved lines(two dimensional) or by flat or curved surfaces(three dimensional).

The shape, size and distribution of the elements are arbitrary. Rectangular, triangular and three dimensional elements could be used efficiently in various studies. In many cases only one type of element is used for one problem, but it is also possible to mix elements of different types. For example for two dimensional steady state finite element formulation both triangular and curved-sided elements are in one specific application(3).

Owing to the suitability of the physical nature of the problem, the finite element formulation made in this thesis is in two dimensional form. The region is divided into three nodal triangular elements due to their simplicity and greater adaptability in fitting boundary geometries.

The governing equation for a transient heat conduction problem as given previously is in the form;

$$\text{div}(k \text{ grad } T) + q - C \frac{\partial T}{\partial t} = 0 \quad (2.16)$$

The mathematical formulation of a physical heat conduction problem is completed with the given dirichlet boundary conditions being prescribed on one part of the boundary and neumann conditions on the remaining part of the boundary. Heat flux and convection loss are also taken into account for some relevant element boundaries for completeness. The region R of the problem consists of the domain D and the boundary S, that is,  $R=D+S$ .

Equation(2.16) and the equations related with the different types of boundary conditions are not employed directly but instead the equivalent variational formulation is used. It can be shown from the calculus of variations(Appendix A) that the solution  $T(x,y)$  satisfying equation(2.16) together with the appropriate boundary conditions is identical to that function which minimizes the functional,

$$\chi = \iint \left\{ \frac{1}{2} k \left[ \left( \frac{\partial T}{\partial x} \right)^2 + \left( \frac{\partial T}{\partial y} \right)^2 \right] - (q - C \frac{\partial T}{\partial t}) T \right\} dx dy \quad (2.17)$$

Where  $T(x,y)$  are admissible trial functions over the domain  $D$ . For this study, the trial functions  $T(x,y)$  are admissible if they are continuous and have piecewise continuous first derivatives in the domain  $D$ . Moreover, the trial functions should satisfy the principal boundary conditions. The Neumann boundary conditions, that is, boundary conditions for which the normal gradient  $\frac{\partial T}{\partial n}$  is zero at the boundary, are satisfied automatically by that function minimizing the functional in equation(2.17) as a natural consequence of the variational procedure. For this reason Neumann boundary conditions are also called as natural boundary conditions.

When there is a constant heat flux per unit area of the boundary surface or a convective loss at the boundary, the energy functional takes the following form;

$$\chi = \iint \left\{ \frac{1}{2} k \left[ \left( \frac{\partial T}{\partial x} \right)^2 + \left( \frac{\partial T}{\partial y} \right)^2 \right] - (q - C \frac{\partial T}{\partial t}) T \right\} dx dy - \int_C q \cdot T \, ds + \int_C \alpha \left( \frac{1}{2} T^2 - T_a T \right) ds \quad (2.18)$$

The last two terms(integrals) in equation(2.18) are taken along the boundary.

As the next step the two dimensional region for which the solution is sought is divided into sufficient number of elements(three nodal triangular) as represented in Fig.2.3.

As a consequence of the division of the region into finite

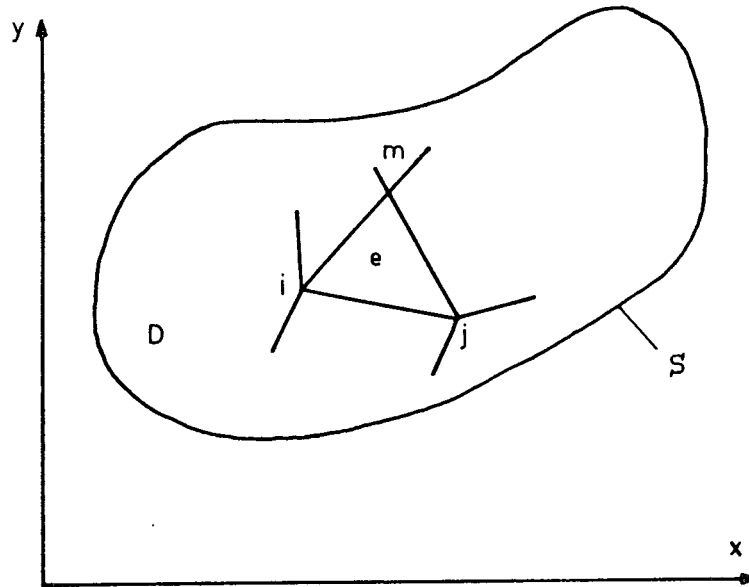


FIGURE 2.3 Division of region into elements.

elements some definite number of nodes are generated. The total number of these nodes which are actually the corners of the triangular elements do not have any obvious relationship with the total number of elements.

The typical triangular element 'e' shown in Fig.2.3 has three nodes to which node identifiers i,j,and m are assigned in a counter-clockwise manner.The importance of such an assignment will be explained in subsequent chapters.

The next procedure is to choose a trial function  $T^e(x,y)$  for the arbitrary element 'e'. Inside each element the temperature T may be uniquely specified as a linear function of the three nodal temperatures  $T_i, T_j, T_m$ . Thus for each element the following relationship can be written using matrix notation;

$$T = [N_i, N_j, N_m] \begin{bmatrix} T_i \\ T_j \\ T_m \end{bmatrix} = [N] [T^e] \quad (2.19)$$

Where  $[T^e]$  means the listing of the nodal temperatures for a particular element and  $[N]$  is called as shape functions for the particular problem.

### 2.2.1 Shape functions

From the last paragraph of the former section it can be concluded that the value of the dependent variable at any point within an element is determined uniquely by the values of the variable at the nodes of the element. All trial functions satisfying the functional could be related with the nodal variables by using suitable shape functions.

The choice of the suitable shape function depends on the person who formulates the finite element procedure. But this choice is the most important part of the whole procedure. A good shape function will lead to an element of high accuracy and with converging characteristics, and conversely a wrongly chosen shape function resulting poor or non-converging results.

The shape functions of two dimensional elements are given in terms of several polynomials(7). The efficiency of the shape functions depends on the degree of the polynomial selected. Lagrange polynomials, hermitian polynomials are the examples of the polynomials used in shape functions. Certainly the choice of any polynomial is also closely related with the nature of the problem.

All these mentioned shape functions using polynomials of different types and orders are concerned with cartesian (x,y) coordinates and generally applicable to rectangular elements. For general quadrilateral elements with straight or curved sides, similar functions can be used but in order

to make the solution possible some further transformation to another coordinate system (curvilinear  $[\xi, \eta]$ ) is necessary (3).

### 2.2.2 Area coordinates

The cartesian coordinates are not much convenient for triangular elements either. Hence, in this work a special type of coordinate system called area coordinates (or natural coordinates) are used instead of the well-known cartesian coordinate system. It will be clearly evident as proceeding further that the use of the area coordinate system enables us to formulate element shape functions and to integrate the resultant functionals much more easily.

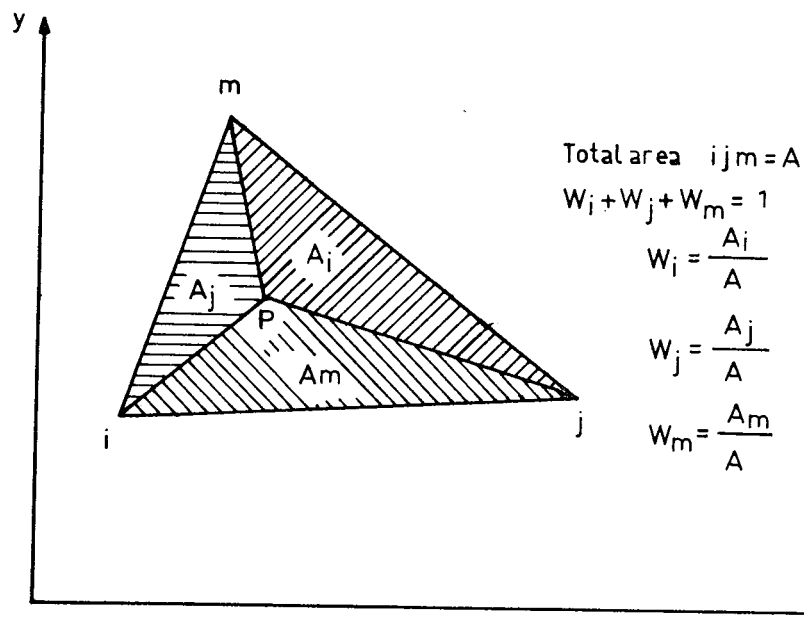


FIGURE 2.4 A triangle and the area coordinate system.

Referring to Fig.2.4 it is seen that the internal point 'p' will divide the triangle (ijm) into three smaller triangles, and depending on the position of the point 'p', the area of each one of the triangles 'pim', 'pij' and 'pmj' can vary from zero to 'A', which is the area of the triangle 'ijm'. In other words, the ratios  $A_i/A$ ,  $A_j/A$  and  $A_m/A$  will take

up any value between zero and unity in the same way as a first order lagrange polynomial. These ratios are called area coordinates, and they are defined by;

$$\begin{aligned}\omega_i &= \frac{A_i}{A} = (a_i + b_i x + c_i y) / 2A \\ \omega_j &= \frac{A_j}{A} = (a_j + b_j x + c_j y) / 2A \\ \omega_m &= \frac{A_m}{A} = (a_m + b_m x + c_m y) / 2A\end{aligned}\tag{2.20}$$

in which,

$$\begin{aligned}a_i &= x_j y_m - x_m y_j \\ b_i &= y_j - y_m \\ c_i &= x_m - x_j\end{aligned}\tag{2.21}$$

$$2A = \det \begin{vmatrix} 1 & x_i & y_i \\ 1 & x_j & y_j \\ 1 & x_m & y_m \end{vmatrix} = 2x(\text{area of triangle 'ijm'})$$

$x_i, y_i$ , etc. are the nodal coordinates and  $a_j, b_j, c_j$  etc. can be computed through a cyclic permutation of the subscripts.

From equation(2.20) a relation between area coordinates and cartesian coordinates may be derived in a matrix form;

$$\begin{bmatrix} \omega_i \\ \omega_j \\ \omega_m \end{bmatrix} = \frac{1}{2A} \begin{bmatrix} a_i & b_i & c_i \\ a_j & b_j & c_j \\ a_m & b_m & c_m \end{bmatrix} \begin{bmatrix} 1 \\ x \\ y \end{bmatrix} \quad (2.22)$$

Solving for 1, x, y we obtain the inverse relation;

$$\begin{bmatrix} 1 \\ x \\ y \end{bmatrix} = \begin{bmatrix} 1 & 1 & 1 \\ x_i & x_j & x_m \\ y_i & y_j & y_m \end{bmatrix} \begin{bmatrix} \omega_i \\ \omega_j \\ \omega_m \end{bmatrix} \quad (2.23)$$

The resultant functions  $\omega_i$ ,  $\omega_j$  and  $\omega_m$  are the linear shape functions relating the nodal variables with the value of the dependent variable at any point within the element. In vector notation the shape function for an element is given as,

$$N = \begin{bmatrix} \omega_i, \omega_j, \omega_m \end{bmatrix} \quad (2.24)$$

This shape function is a linear first order relation which is valid for a simple three nodal triangular element. For higher order quadratic and cubic triangular elements the related higher order shape functions derived from area coordinates are given in the (Appendix B) for information.

When element matrices have to be evaluated we will be faced with integration of quantities defined in terms of area coordinates over the triangular region. The values of these integrals are independent of the shape and the location of the triangles in the cartesian coordinate system because of the special properties of the area coordinates chosen.

In general, the element contributions will then involve integrals of the form  $\int_A \omega_i^n \omega_j^r \omega_m^s dA$  which can be evaluated

analytically through the relation(2),

$$I = \int_A \omega_i^n \omega_j^r \omega_m^s dA = 2A \frac{n! r! s!}{(n+r+s+2)!} \quad (2.25)$$

### 2.2.3 Application of finite element method to thermal transient problems

As previously indicated by the equation(2.19) temperature  $T$  at any point inside an triangular element may be uniquely specified as a linear function of the three nodal temperatures  $T_i, T_j$  and  $T_m$ . In the same manner the first time derivatives of the temperature  $T$  can be specified as a linear function of the time derivatives of the nodal temperatures. Thus within an element;

$$\frac{\partial T}{\partial t} = [N_i, N_j, N_m] \begin{bmatrix} \frac{\partial T_i}{\partial t} \\ \frac{\partial T_j}{\partial t} \\ \frac{\partial T_m}{\partial t} \end{bmatrix} = [N] \left[ \frac{\partial T^e}{\partial t} \right] \quad (2.26)$$

Substituting equation(2.26) and equation(2.19) into equation(2.17) and integrating over an element gives functional (thermal energy)  $\chi_e$  of the element in terms of the nodal temperatures  $T_i, T_j$  and  $T_m$ .

The total thermal energy or the functional  $\chi$  can be expressed as the sum of the  $\chi_e$  values of each element.

$$\chi = \sum \chi^e \quad (2.27)$$

For this equation to hold true the temperature  $T$  must be continuous along the element boundaries. This of course has been ensured by the appropriate selection of shape functions.

The solution of the transient heat conduction problem given as a parabolic partial differential equation (equation 2.16) reduces to finding the nodal temperatures which minimise the energy functional(2.27). This can be achieved by minimizing the functional  $\chi_e$  for each element.



### 2.2.3.1 Energy minimization of one element

In the light of area coordinates introduced in previous sections the temperature  $T$  at any point within an element is given as;

$$T = \omega_i T_i + \omega_j T_j + \omega_m T_m = [N][T^e] \quad \text{where, } N = [\omega_i \quad \omega_j \quad \omega_m] \text{ is the shape function, in the same way, } \frac{\partial T}{\partial t} = \omega_i \frac{\partial T_i}{\partial t} + \omega_j \frac{\partial T_j}{\partial t} + \omega_m \frac{\partial T_m}{\partial t} = N \frac{\partial T^e}{\partial t}$$

The relations between area coordinates and the coordinates given previously by equations(2.22) and (2.23) indicates that only two of the area coordinates are independent. Let these be  $\omega_i$  and  $\omega_j$ . The relation between temperature derivatives with respect to area coordinates and temperature derivatives with respect to cartesian coordinates is;

$$\begin{bmatrix} \frac{\partial T}{\partial x} \\ \frac{\partial T}{\partial y} \end{bmatrix} = J \begin{bmatrix} \frac{\partial T}{\partial \omega_i} \\ \frac{\partial T}{\partial \omega_j} \end{bmatrix} \quad (2.28)$$

Where  $J$  is the jacobian matrix. The following can easily be derived from previous relations as;

$$J = \frac{1}{2A} \begin{bmatrix} y_j - y_m & y_m - y_i \\ x_m - x_j & x_i - x_m \end{bmatrix} = \frac{1}{2A} \begin{bmatrix} b_i & b_j \\ c_i & c_j \end{bmatrix} \quad (2.29)$$

Since  $\omega_i$  and  $\omega_j$  are selected as two independent area coordinates  $\omega_m$  can be defined in terms of these coordinates, i.e;

$$\omega_m = 1 - \omega_i - \omega_j \quad (2.30)$$

Hence the relation between temperature derivatives and nodal temperatures is found using the equality given by equation(2.30) and by differentiating equation(2.19),

$$\begin{bmatrix} \frac{\partial T}{\partial \omega_i} \\ \frac{\partial T}{\partial \omega_j} \end{bmatrix} = \begin{bmatrix} 1 & 0 & -1 \\ 0 & 1 & -1 \end{bmatrix} \begin{bmatrix} T_i \\ T_j \\ T_m \end{bmatrix} = [V][T^e] \quad (2.31)$$

Substituting equation(2.31) into equation (2.28) gives,

$$\begin{bmatrix} \frac{\partial T}{\partial x} \\ \frac{\partial T}{\partial y} \end{bmatrix} = [J][V][T^e] \quad [D]=[J][V] \quad (2.32)$$

Substituting this equation into equation(2.17), the energy functional takes the form,

$$\chi^e = \int_A \left\{ \frac{1}{2} k ((DT^e)^t DT^e) - T(q - C \frac{\partial T}{\partial t}) \right\} dA \quad (2.33)$$

The superscript 't' in equation(2.33) means the transpose of the vector  $DT^e$ .

In order to minimize the functional it is differentiated with respect to three nodal values of the element( $T_i, T_j, T_m$ ). First differentiation of  $\chi^e$  with respect to  $T_i$  gives,

$$\frac{\partial \chi^e}{\partial T_i} = \int_A \left\{ k \frac{\partial (DT^e)^t}{\partial T_i} DT^e - \frac{\partial T}{\partial T_i} (q - C \frac{\partial T}{\partial t}) \right\} dA \quad (2.34)$$

Substituting equation(2.19), (2.26) and (2.32) into equation(2.34) gives,

$$\frac{\partial \chi^e}{\partial T_i} = \int_A \left\{ k \frac{\partial [T^e]^t}{\partial T_i} V^t J^t JVT^e - \frac{\partial [T^e]^t}{\partial T_i} [N^t q - N^t CN \frac{\partial T^e}{\partial t}] \right\} dA \quad (2.35)$$

In equation(2.35),

$$\frac{\partial [T^e]^t}{\partial T_i} = [1, 0, 0]^t$$

Following the same procedure for the differentiation of  $\chi^e$  with respect to all nodal values  $T_i, T_j$  and  $T_m$ , the resultant equation will be,

$$\begin{bmatrix} \frac{\partial \chi^e}{\partial T_i} \\ \frac{\partial \chi^e}{\partial T_j} \\ \frac{\partial \chi^e}{\partial T_m} \end{bmatrix} = \int_A \left\{ kV^t J^t JVT^e + CN^t N \frac{\partial T^e}{\partial t} - N^t q \right\} dA \quad (2.36)$$

The first term in the integral(2.36) is constant over the area of the element. Substituting the values of V and J the first term of the integral becomes;

$$(kV^t J^t J^t \int_A d\Lambda) T^e =$$

$$\frac{k}{4A} \begin{bmatrix} 1 & 0 \\ 0 & 1 \\ -1 & -1 \end{bmatrix} \begin{bmatrix} b_i & c_i \\ b_j & c_j \end{bmatrix} \begin{bmatrix} b_i & b_j \\ c_i & c_j \end{bmatrix} \begin{bmatrix} 1 & 0 & -1 \\ 0 & 1 & -1 \end{bmatrix} \begin{bmatrix} T_i \\ T_j \\ T_m \end{bmatrix} \quad (2.37)$$

Using the relations  $(c_i+c_j)=-c_m$  and  $(b_i+b_j)=-b_m$  equation(2.37) takes the following form;

$$h^e T^e = \frac{k}{4A} \begin{bmatrix} b_i^2+c_i^2 & b_i b_j+c_i c_j & b_i b_m+c_i c_m \\ b_i b_j+c_i c_j & b_j^2+c_j^2 & b_j b_m+c_j c_m \\ b_i b_m+c_i c_m & b_j b_m+c_j c_m & b_m^2+c_m^2 \end{bmatrix} \begin{bmatrix} T_i \\ T_j \\ T_m \end{bmatrix} \quad (2.38)$$

$h^e$  in equation(2.38) is called as the heat conductivity matrix for one element.

The second term in the integral(2.36) is,

$$[p^e] \left[ \frac{\partial T^e}{\partial t} \right] = \int_A C N^t N dA = C \int_A \begin{bmatrix} \omega_1^2 & \omega_1 \omega_j & \omega_1 \omega_m \\ \omega_1 \omega_j & \omega_j^2 & \omega_j \omega_m \\ \omega_1 \omega_m & \omega_j \omega_m & \omega_m^2 \end{bmatrix} dA \quad (2.39)$$

Equation(2.39) contains integrals of the form given in the equation(2.25). Using the equality given in equation(2.25) the integrals of each element of the matrix given in (2.39) can easily be taken over the element area.

$$[P^e] \left[ \frac{\partial T^e}{\partial t} \right] = \frac{C A}{12} \begin{bmatrix} 2 & 1 & 1 \\ 1 & 2 & 1 \\ 1 & 1 & 2 \end{bmatrix} \left[ \frac{\partial T^e}{\partial t} \right] \quad (2.40)$$

The matrix  $[P^e]$  in (2.40) is called as the heat capacity matrix for one element.

The last integral term in equation(2.36) is,

$$K^e = \int_A N^t q dA = q \int_A \begin{bmatrix} \omega_1 \\ \omega_2 \\ \omega_3 \end{bmatrix} dA = \frac{qA}{3} \begin{bmatrix} 1 \\ 1 \\ 1 \end{bmatrix} \quad (2.41)$$

Here the integral is evaluated again using the identity given by (2.25). Another point is that heat generation 'q' is assumed to be evenly distributed within the element hence it is taken as a constant over the element area.  $[K^e]$  in equation(2.41) is called as heat generation vector. Finally, equation(2.36) after evaluating all integral terms becomes the following form;

$$\left\{ \frac{\partial \chi}{\partial T_n} \right\}^e = h^e T^e + P^e \frac{\partial T^e}{\partial t} - K^e \quad (2.42)$$

### 2.2.3.2 Assembly of elements

Equation(2.42) is the differentiation of the functional  $\chi^e$  of one element with respect to the nodal values.

The next step is to equate this equation to zero to find the minimum of the energy functional. According to the variational

approach the finite element solution of the problem is obtained by finding the nodal temperatures which minimise the energy functional  $\chi = \sum \chi^e$

Therefore the process done for one element is carried out for all elements. After rearranging, the final set of equations can be written as,

$$\left[ \frac{\partial \chi}{\partial T_n} \right] = \sum \left[ \frac{\partial \chi}{\partial T_n} \right] = [H][T] + [P] \left[ \frac{\partial T}{\partial t} \right] - [K] = 0 \quad (2.43)$$

In this equation  $[H]$  is the heat conductivity matrix,  $[P]$  the heat capacity matrix,  $[T]$  and  $\left[ \frac{\partial T}{\partial t} \right]$  are vectors containing the nodal temperatures and their time derivatives respectively.  $[K]$  is the vector defining the distribution of heat sources and heat sinks over the region under consideration.

Observation of equation(2.43) reveals that in order to proceed with the transient part of the solution another numerical approximation procedure is required. When solving (2.43),  $\left[ \frac{\partial T}{\partial t} \right]$  is to be substituted by a finite difference. There are basically three finite difference approximations in dealing with the transient part of the finite element problem.

These are Euler, Crank-Nicolson, and pure implicit methods. In the Euler method the solution is advanced in time by the relation,

$$[T]_t = [T]_{t-\Delta t} + \Delta t \left[ \frac{\partial T}{\partial t} \right]_{t-\Delta t}$$

On the other hand the Crank-Nicolson method moves the solution ahead in time according to the relation,

$$[T]_t = [T]_{t-\Delta t} + \left( \left[ \frac{\partial T}{\partial t} \right]_{t-\Delta t} + \left[ \frac{\partial T}{\partial t} \right]_t \right) \frac{\Delta t}{2} \quad (2.44)$$

And finally pure implicit method moves the solution ahead in time as follows,  $[T]_t = [T]_{t-\Delta t} + \Delta t \left[ \frac{\partial T}{\partial t} \right]_t$

In this work Crank-Nicholson approximation is used since it provides better results, at least upon Euler's method as proved by experience(8).

The equation(2.44) considered with the equation(2.43) gives the simultaneous time and space solution for the transient heat conduction problem.

The algorithm proposed for this part of the problem is as follows(9).

At time 't' , substituting equation(2.44) into equation(2.43) following relation is obtained.

$$\left( \frac{2}{\Delta t} [P] + [H] \right) [T]_t = [P] \left( \left[ \frac{\partial T}{\partial t} \right]_{t-\Delta t} + \frac{2}{\Delta t} [T]_{t-\Delta t} \right) + [K] \quad (2.45)$$

This time substituting equation(2.43) into equation (2.45) at time '(t- Δt)' ;

$$\left( \frac{2}{\Delta t} [P] + [H] \right) [T]_{t-\Delta t} = \left( [P] \frac{2}{\Delta t} - [H] \right) [T]_{t-\Delta t} + 2 [K] \quad (2.46)$$

Defining;

$$\begin{aligned} [H]^* &= [P] \frac{2}{\Delta t} + [H] \\ [K]^* &= [K] + \frac{2}{\Delta t} [P] [T]_{t-\Delta t} \\ [H]^* [T]^* &= [K]^* \end{aligned} \quad (2.47)$$

Following the above procedure first  $[T]^*$  's are determined then solving the equation given below the nodal tem-

peratures at time 't' is found if the initial conditions at  $t-\Delta t$  are given;

$$[T]_t = 2 [T]^* - [T]_{t-\Delta t}$$

The time step  $\Delta t$  is chosen appropriately and the continuous solution of the time dependent problem is obtained at each time interval.

### 2.2.3.3 Mathematical consideration of boundary conditions in the solution of the time dependent problem

As mentioned previously in section(2.1.2) depending to the type of the problem different types of Boundary conditions should be taken into account when solving the specific problem. When considering boundary conditions the energy functional of the system takes the mathematical form given by (2.18) in which the last two terms related with the boundary conditions are integrated along the element boundaries.

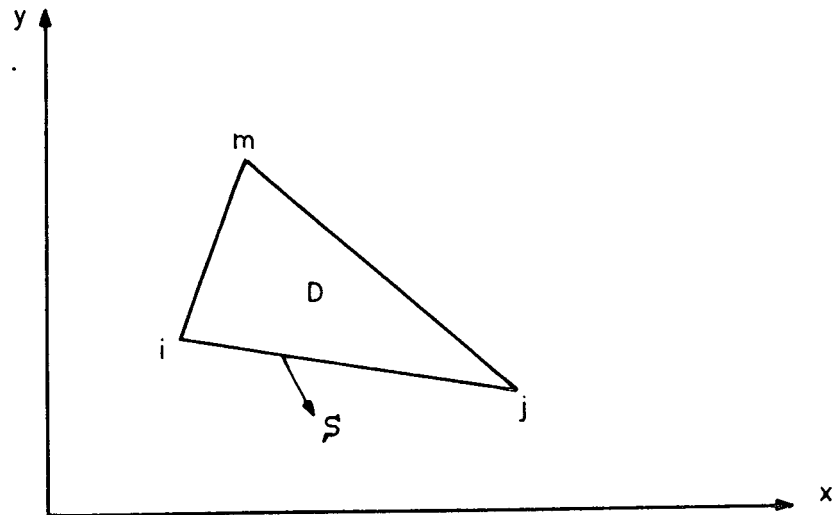


FIGURE 2.5 Consideration of boundary conditions.

Suppose that for the element indicated in Fig.2.5 all boundary conditions represented by the last two terms of equation(2.18) are valid for the side 'ij'. In other words for the side 'ij' both constant heat flux per unit area and convection loss

are considered to be valid.

From the knowledge of area coordinates it can be concluded that  $\omega_m = 0$  along side 'ij'.

Since  $\omega_i + \omega_j + \omega_m = 1$

and  $\omega_m = 0$

$\omega_i = 1 - \omega_j$  can be written.

also letting  $\omega_j = \frac{s}{d}$  where d is the distance between i and j, and s is the distance measured from node i ;

The temperature can be expressed as

$$T = T_i + (T_j - T_i)\omega_j = T_i + (T_j - T_i)\frac{s}{d} \quad (2.48)$$

Temperature distribution along the element boundary S can be found by the minimum of the last two terms of energy functional given by (2.18). This can be achieved by taking the derivatives with respect to nodal temperature parameter and equating to zero.

First taking with respect to  $T_i$ ,

$$\begin{aligned} \frac{\partial}{\partial T_i} [ \int_0^d \alpha (\frac{T^2}{2} - TT_a) ds - \int_0^d QT ds ] = \\ \alpha \int_0^d (T \frac{\partial T}{\partial T_i} - \frac{\partial T}{\partial T_i} T_a) ds - Q \int_0^d \frac{\partial T}{\partial T_i} ds \end{aligned} \quad (2.49)$$

Substituting equation(2.48) into equation(2.49) and setting

$$\frac{\partial T}{\partial T_i} = (1 - \frac{s}{d}) \quad ;$$

$$\begin{aligned} \alpha \int_0^d [ (T_i + \frac{T_j - T_i}{d} s)(1 - \frac{s}{d}) - (1 - \frac{s}{d}) T_a ] ds \\ - Q \int_0^d (1 - \frac{s}{d}) ds = \frac{\alpha d}{3} T_i + \frac{\alpha d}{6} T_j - \frac{\alpha d}{2} T_a - Q \frac{d}{2} \end{aligned} \quad (2.50)$$



In the like manner for  $T_j$  gives

$$\frac{\alpha d}{3} T_j + \frac{\alpha d}{6} T_i - \frac{\alpha d}{2} T_a - \left(\frac{d}{2}\right) \quad (2.51)$$

As it is evident from equations (2.50) and (2.51) the coefficients of nodal Temperature values  $T_i$  and  $T_j$  must be inserted into suitable places in equation (2.43). These results are only for one element boundary. Repeating the process for all elements which have prescribed boundary conditions, the similar results are obtained and all of them are inserted to equation (2.43) in a systematic way.

According to the equations (2.50) and (2.51) the coefficients  $h_{ii}$  and  $h_{jj}$  in the  $[H]$  matrix are increased by  $\frac{\alpha d}{3}$ , while the terms  $h_{ij}$  and  $h_{ji}$  is increased by  $\frac{\alpha d}{6}$ . On the other hand to the elements  $i$  and  $j$  of vector  $[K]$  will be added  $(\frac{\alpha d}{2} T_a + \frac{d}{2})$ .

Dirichlet boundary conditions may be taken into consideration in one of several ways. If dirichlet kind of boundary conditions are prescribed for one part of the boundary the insertion of them into appropriate places of the equation (2.43) may create some problems. Depending upon the method chosen the symmetric and banded nature of the  $[H]$  matrix may greatly be destroyed. Several methods (7) are proposed and one which does not affect the nature of the  $[H]$  matrix is selected in this study. The method has also some other advantages over the others such as it requires very few operations.

Dirichlet boundary condition is taken into care at the stage given by the equation (2.47),

$$[H]^* [T]^* = [K]^*$$

Supposing 'A' is the value given by dirichlet boundary con-

dition, then in this method, the diagonal coefficient corresponding to  $T_n^*$  is multiplied by a very large number ( $10^{12}$  is selected in this study), and the term  $K_n^*$  is replaced by  $Ax_{nn} \times 10^{12}$ .

The modified equations are shown below;

$$\begin{bmatrix} h_{11} & h_{12} \cdot \cdot \cdot h_{1n} \cdot \cdot \cdot h_{1N} \\ h_{21} & h_{22} \cdot \cdot \cdot h_{2n} \cdot \cdot \cdot h_{2N} \\ \vdots & \vdots \\ h_{n1} & h_{n2} \cdot \cdot \cdot h_{nn} \times 10^{12} \cdot h_{nN} \\ \vdots & \vdots \\ h_{N1} & h_{N2} \cdot \cdot \cdot \cdot \cdot h_{NN} \end{bmatrix}^* \begin{bmatrix} T_1 \\ T_2 \\ \vdots \\ T_n \\ \vdots \\ T_N \end{bmatrix}^* = \begin{bmatrix} k_1 \\ k_2 \\ \vdots \\ Ax_{nn} \times 10^{12} \\ \vdots \\ k_N \end{bmatrix}^*$$

It is obvious that the dirichlet boundary value ' A ' given for node ' n ' has been taken into account in this way, that is, the solution of the above set of algebraic equations gives nearly equal to  $T_n = A$ .

CHAPTER III  
SOME PRACTICAL ASPECTS OF FINITE ELEMENT METHOD  
AND PROGRAM DEVELOPMENT

In chapter II an outline of the finite element method and the detailed formulation of the mathematical equations for solving a transient heat conduction problem were introduced. Now, in this chapter some practical aspects of finite analysis which are to be considered in developing a computer program will be represented. A flow chart of the developed program is given at the end of the chapter.

3.1 Modelling of a problem.

A two dimensional solution domain in which transient heat distribution is sought for is divided into finite number of triangular elements. Associated with each element are three nodal points, at the corners of the triangle. The triangular elements are utilised so that they can be made to fit any shape of the domain boundary. Boundary is represented with sufficient accuracy by a series of short lines.

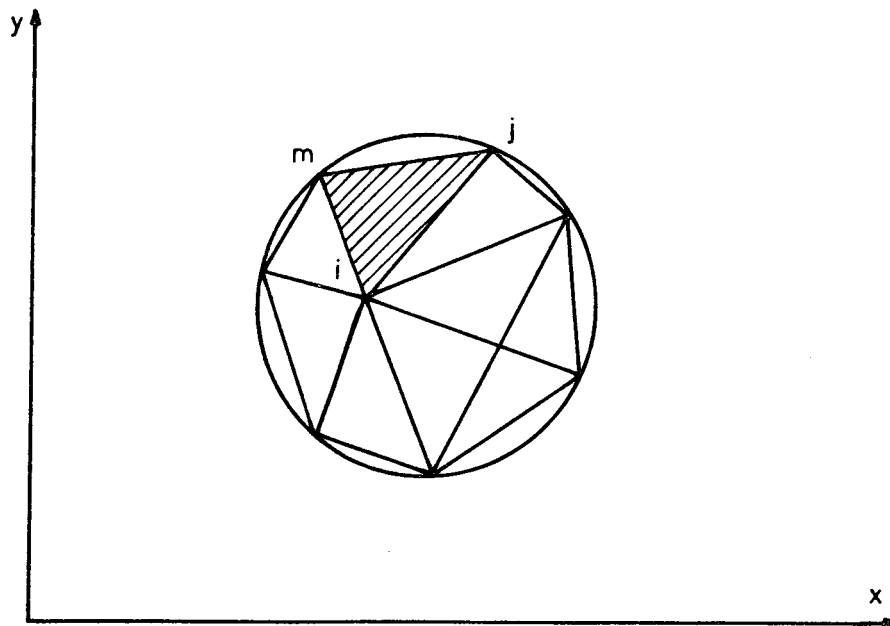


FIGURE 3.1 A twodimensional circular solution domain divided into triangular finite elements.

Each element has common edges with the other ones, but each edge is allowed to be common between two neighbouring elements at most, as indicated in Fig.3.1. Otherwise, a division of the region as shown in Fig.3.2 is not allowed.

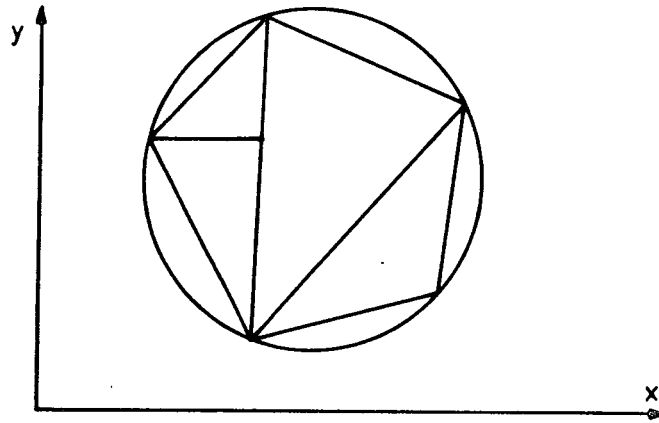


FIGURE 3.2 An incorrect division.

Element divisions are made appropriately, considering the different material properties of the different subregions of the solution domain.

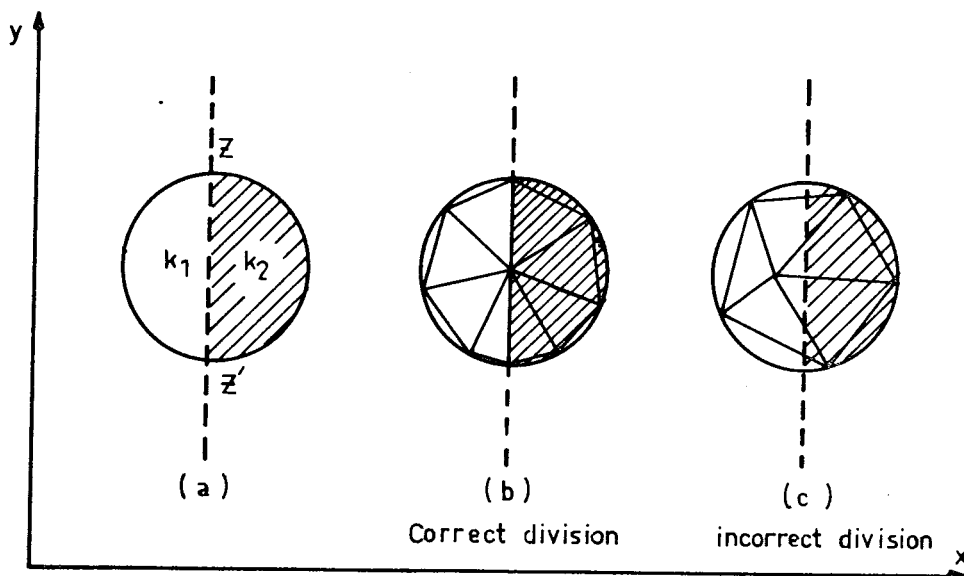


FIGURE 3.3 Division of a region with differing material properties.

As an example, Fig.3.3-a shows a solution domain composed of two subregions divided by vertical  $zz'$  axis having two different heat conductivities  $k_1$  and  $k_2$

As a result of a division shown in Fig.3.3-c the solution is not possible, since some of the elements are allocated partly in one region and partly in the other having different material properties.

The Fig.3.4 makes it simple to follow the subsequent steps when modelling the finite element method. It represents a two dimensional solution domain of a simple geometry.

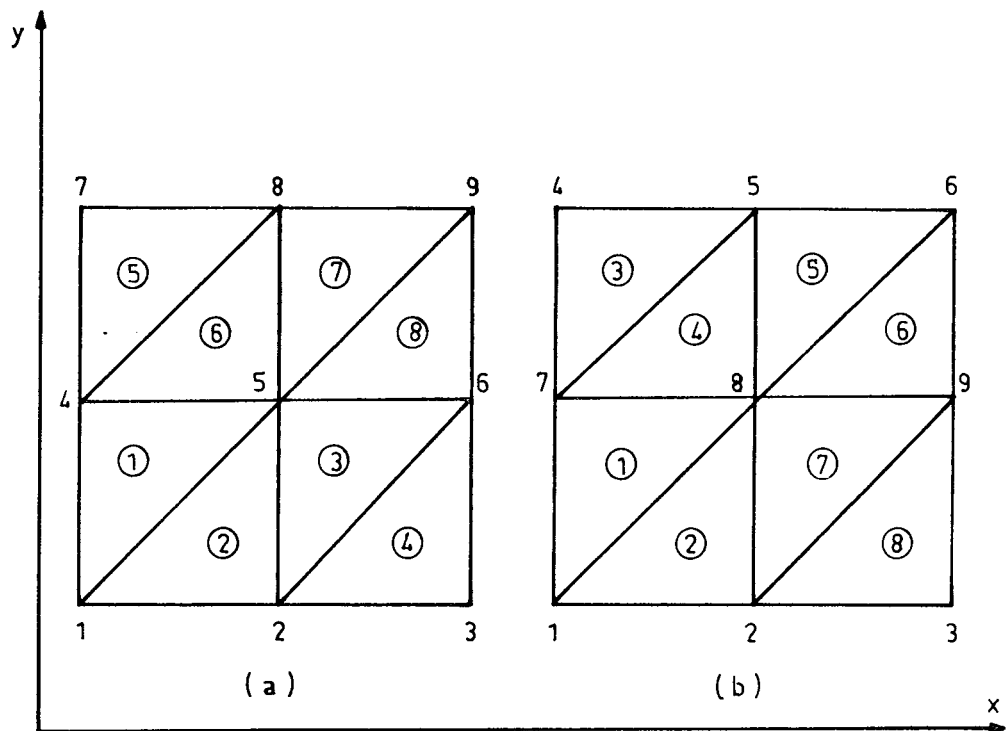


FIGURE 3.4 Element and node numbering.

As the division of the region into finite number of elements is completed then the number of nodes and elements are

to be determined. The region in Fig.3.4 have 9 nodes and 8 elements totally. It is clear that for any particular geometry other than the one given in this figure, there is no obvious relation between the number of nodes and the number of elements.

Table 3.1 relates the node identifiers i, j, m of each element to the system node numbers.

Element	Node Number		
	i	j	m
1	1	5	4
2	2	5	1
3	2	6	5
4	3	6	2
5	4	8	7
6	5	8	4
7	5	9	8
8	6	9	5

Table 3.1 Relationship between node numbers and element node identifiers

As an investigation on both table 3.1 and Fig.3.4 reveals that the node identifiers are allocated in a counter-clockwise manner on each element. Such a systematic pattern prevents an appearance of a negative element area which certainly would cause the mathematical formulation given in previous chapter to yield wrong results.

The elements are numbered in a sequential order from bottom row up to the next as shown in Fig.3.4. However, this is not a requirement so that the elements could as well be numbered in any other manner as someone wishes.

### 3.1.1 Node numbering and Bandwidth

Node numbering of a finite element is one of the most important part of the whole procedure. Fig.3.4-a and b shows same finite element mesh with two different node numbering. The importance of node numbering comes from the fact that matrices generally met in finite element problems have a banded nature. In the matrices  $[H]$  and  $[P]$  derived in chapter II; the non-zero coefficients are usually cumulated near the diagonal, and outside this band all the coefficients are of zero value. Such matrices are called as banded matrices. In most of the finite element problems, the nodes are numbered sensibly so that the matrices become banded. This banded nature of the matrices offers a great advantage in programming finite element problems especially for storage requirement of computers. The core requirement is directly proportional to the halfband-width which is in turn related to the maximum difference between the nodal numbers of an element. Therefore when numbering nodes great care must be exercised so that the difference between connecting nodes can be minimised. Fig.3.5-a and b represents the form of the system matrix obtained in respect to the two different numbering schemes introduced in Fig.3.4 -a and b respectively. The matrix in Fig.3.5-a is a fairly compact one, on the other hand, by numbering the nodes incorrectly associated with the Fig.3.4-b, the matrix is no longer banded and almost entire system matrix should be in the solution process.

Since the time and the cost of the solution is closely dependent upon the bandwidth, a great advantage will be lost if the nodes are numbered as in Fig.3.4-b. Therefore it is desirable to number the nodes in such a way that the bandwidth is minimized. This purpose can easily be achieved for simple geometries, but this may not be the case

X	X	O	X	X	.	.	.	.
X	X	X	O	X	X	.	.	.
O	X	X	O	O	X	.	.	.
X	O	O	X	X	O	X	X	.
X	X	O	X	X	X	O	X	X
.	X	X	O	X	X	O	O	X
.	.	.	X	O	O	X	X	.
.	.	.	X	X	O	X	X	X
.	.	.	.	X	X	O	X	X

-a-

X	X	O	O	O	O	X	X	.
X	X	X	O	O	O	O	X	X
.	X	X	O	O	O	O	O	X
.	.	.	X	X	O	X	.	.
.	.	.	X	X	X	O	X	.
.	.	.	.	X	X	O	X	X
X	O	O	X	X	O	X	X	.
X	X	O	O	X	X	X	X	X
.	X	X	O	O	X	O	X	X

-b-

Figure.3.5 Matrix forms for different node numbering



for complex geometries. Some numbering algorithms are developed for complex geometries using the data of already numbered region and renumber the nodes so that bandwidth is minimized(10).

### 3.1.2 Automatic mesh generation

One of the data input sets of a finite element program is the listing of x and y coordinates of the nodes. But for problems with large numbers of elements, the preparation of data; including the determination of x and y coordinates of all nodes, element numbers and node identifiers associated with each element number, can be tedious and time consuming. Ideally, a finite element computer program should generate its own mesh data from a minimum number of geometric parameters. The amount of input data required is minimum and once the relevant routine has been written by this way the possibility of errors is largely eliminated. Although an automatic mesh generation provides a powerful tool in handling data preparation for finite element programs it is not so simple to device algorithms suitable for all kinds of geometries. In this work an automatic mesh generation subroutine has been used in one of the applications of the finite element program to a problem having relatively simple geometry.

The automatic mesh generation scheme is devised for the geometry shown in Fig.4.1 in chapter IV. For this purpose a square mesh with the same number of elements and nodal points is chosen (Fig.3.6)

First an algorithm generating this geometry is devised.

Considering the general case where there are  $n_x$  points per horizontal row and  $n_y$  points per vertical row, the total numbers of nodes and elements are  $n_x n_y$  and  $2(n_x - 1)(n_y - 1)$  respectively.

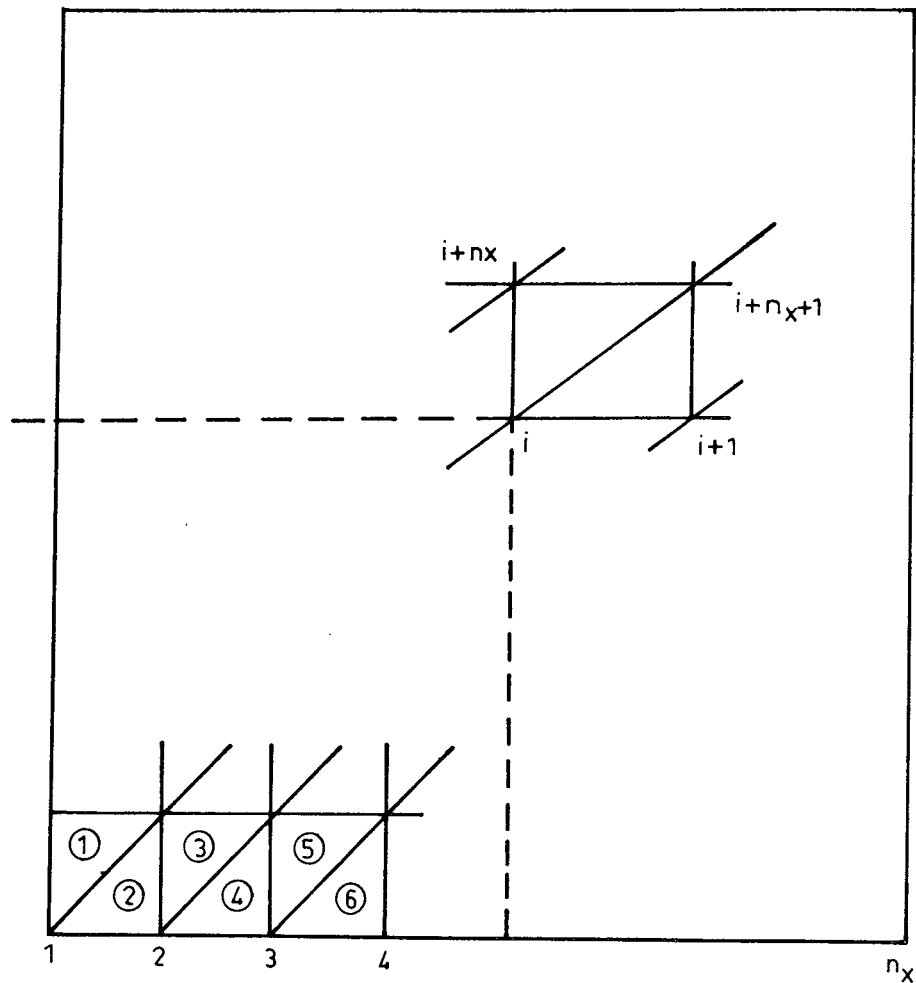


FIGURE 3.6 A square mesh with right angled triangular elements.

Let  $i_x$  be used to count nodes from left to right in a specific horizontal row and  $i_y$  be used to count such rows from the bottom to the top, where  $1 \leq i_x \leq n_x$  and  $1 \leq i_y \leq n_y$ . Since the order of node numbering is from left to right as shown in Fig.3.6 then the number of any node can be obtained as follows,

$$i = (i_y - 1)n_x + i_x$$

The dimensions of the mesh in both x and y directions are taken as unity. And the origin of the coordinate system is

assumed to be at the node numbered 1. Coordinates of any typical node is then

$$x_i = \frac{i_x - 1}{n_x - 1} \quad , \quad y_i = \frac{i_y - 1}{n_y - 1}$$

Where  $x_i$  and  $y_i$  indicates x and y coordinates of the node i.

The numbers of the nodal points at the corners of each element may be defined by considering the overall mesh to be divided into a total of  $(n_x - 1)(n_y - 1)$  small squares, each one of which is then subdivided into two triangles. This time letting  $i_x$  and  $i_y$  being the horizontal and vertical counters applied to squares, where now  $1 \leq i_x \leq n_x - 1$  and  $1 \leq i_y \leq n_y - 1$ . Since the squares are numbered in an order from left to right in a particular horizontal row then the number of any specific square will be

$$n_q = (i_y - 1)(n_x - 1) + i_x$$

Since there are twice as many elements as there are squares, then the two elements of each square can be numbered as

$$m_1 = 2n_q - 1 \quad m_2 = 2n_q$$

The next step is to number the three nodes of one triangular element in an anticlockwise manner. Let i be the number of the bottom left hand corner of a square, then the numbering of the nodes of the two elements associated with any particular square will be

$$\begin{aligned} i_1 &= i & j_1 &= i + n_x + 1 & , & k_1 &= i + n_x \\ i_2 &= i & j_2 &= i + 1 & , & k_2 &= i + n_x + 1 \end{aligned}$$

By this way all the geometrical data associated with a square mesh composed of right angled triangular elements are obtained.

As a next step another routine which provides a modification to the square mesh, resulting in a geometry similar to that of Fig.4.1 with parallel concentric arcs. To achieve this, the inner and outer radii of the geometry and a constant ratio of radial distances between successive rows of nodes must be given. Let  $h_r$  be the distance between the first two rows of Fig.4.1 and  $S$  be the ratio of the radial distances between rows. Let  $a$  and  $b$  be the inner and outer radii respectively.

Since there are  $n_y$  parallel concentric rows,

$$h_r (1+S+S^2+\dots+S^{n_y-2}) = b-a$$

$$h_r = \frac{(b-a)(S-1)}{S^{n_y-1} - 1} \quad \text{for } S \neq 1$$

the Y coordinates of the original square mesh can be first modified as,

$$Y_i^* = \frac{h_r (S^{i_y-1} - 1)}{S-1}$$

where  $i_y$  is the number of the row in which node  $i$  occurs. Required curvature is introduced using polar coordinates. The modified position of a typical node  $i$  is,

$$r = a + Y_i^* \quad , \quad \theta = \pi x_i$$

and final coordinates are

$$x_i^{**} = r \sin \theta \quad \text{and} \quad y_i^{**} = r \cos \theta$$

By using this algorithm a semi-circular mesh composed of triangular elements as seen in Fig.4.1 is obtained automatically, using very few input data. Altogether the input data to generate such a mesh requires only inner and outer radii of the resulting geometry and a constant ratio of radial distances between circular arcs (or rows).

### 3.2 Solution of simultaneous equations

As it has been derived in chapter 2 the finite element formulation yields a set of linear algebraic equations. These equations are of the following form;

$$AX = B \quad (3.1)$$

Where  $A = [a_{ij}]$  is the coefficient matrix,  $X = [x_j]$  is the system nodal vector of unknowns (nodal temperatures for heat conduction problem) and  $B = [b_j]$  is a vector of known values.

There are several techniques for solving linear systems of equations classified as either direct or iterative methods. In finite element methods the choice of the technique mostly depends on the properties of the matrix A, such as symmetry, bandedness, or sparseness, to reduce the number of computational operations and storage requirements.

In this work two methods; gaussian elimination and square root (Cholesky's) methods are used and compared with each other, at the same time the advantage of the properties of the matrix A is taken into account,

#### 3.2.1 Gaussian elimination using a full matrix

Gaussian elimination is the simplest and most frequently used method of solving a set of simultaneous equations(11). To demonstrate the procedure for this method equation(3.1) is supposed to represent a set of four simultaneous equations.

$$\begin{bmatrix} a_{11} & a_{12} & a_{13} & a_{14} \\ 0 & a_{22} - \frac{a_{21}}{a_{11}} a_{12} & a_{23} - \frac{a_{21}}{a_{11}} a_{13} & a_{24} - \frac{a_{21}}{a_{11}} a_{14} \\ 0 & a_{32} - \frac{a_{31}}{a_{11}} a_{12} & a_{33} - \frac{a_{31}}{a_{11}} a_{13} & a_{34} - \frac{a_{31}}{a_{11}} a_{14} \\ 0 & a_{42} - \frac{a_{41}}{a_{11}} a_{12} & a_{43} - \frac{a_{41}}{a_{11}} a_{13} & a_{44} - \frac{a_{41}}{a_{11}} a_{14} \end{bmatrix} \begin{bmatrix} x_1 \\ x_2 \\ x_3 \\ x_4 \end{bmatrix} = \begin{bmatrix} b_1 \\ b_2 - \frac{a_{21}}{a_{11}} b_1 \\ b_3 - \frac{a_{31}}{a_{11}} b_1 \\ b_4 - \frac{a_{41}}{a_{11}} b_1 \end{bmatrix} \quad (3,2)$$

the reduction or triangularisation of  $[A]$  is carried out by computing,

$$\begin{aligned} a_{ij}^* &= a_{ij} - a_{is} a_{sj} / a_{ss} \\ b_i^* &= b_i - (a_{is} / a_{ss}) b_s \end{aligned} \quad (3.3)$$

and the final form after the completion of all reduction steps is,

$$\begin{bmatrix} a_{11} & a_{12} & a_{13} & a_{14} \\ 0 & a_{22}^* & a_{23}^* & a_{24}^* \\ 0 & 0 & a_{33}^* & a_{34}^* \\ 0 & 0 & 0 & a_{44}^* \end{bmatrix} \begin{bmatrix} x_1 \\ x_2 \\ x_3 \\ x_4 \end{bmatrix} = \begin{bmatrix} b_1 \\ b_2^* \\ b_3^{**} \\ b_4^{***} \end{bmatrix} \quad (3.4)$$

in which asterisks indicate the number of times each coefficient has been modified. Using (3.4) backsubstitution process is carried on and unknown values of vector  $[x]$  is evaluated. This algorithm is certainly inefficient interms of core storage and computer time because no advantage has been taken of the symmetric and banded nature of the  $[A]$  matrix.

### 3.2.2 Gaussian elimination for a banded matrix

As previously mentioned the matrices generally met in finite element problems are symmetric, banded and positive definite matrices.

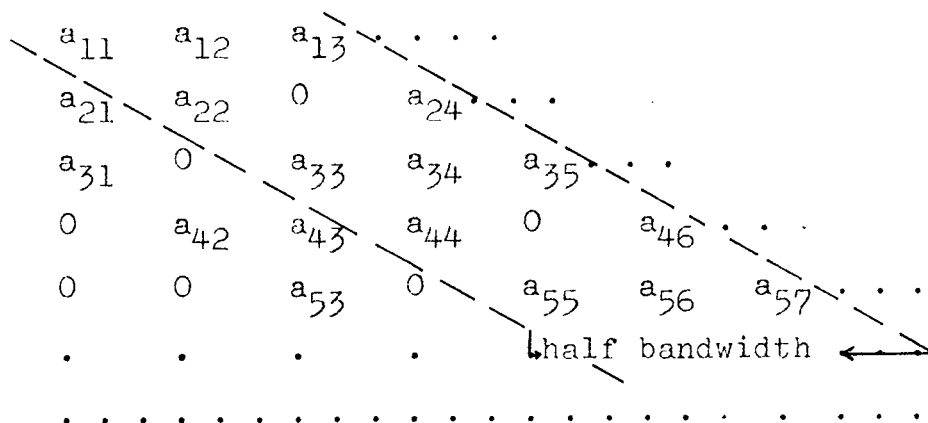


Figure.3.7-a Original band matrix

$$\begin{vmatrix} a_{11} & a_{12} & a_{13} \\ a_{22} & 0 & a_{24} \\ a_{33} & a_{34} & a_{35} \\ a_{44} & 0 & a_{46} \\ a_{55} & a_{56} & a_{57} \end{vmatrix}$$

Figure.3.7-b Rectangular array storage of upper half of the band.

Fig.3.7 shows an alternative way of storing the elements of [A] matrix having a symmetric and banded nature. Using slightly modified routine extra efficiency is gained providing comparatively low storage requirement and reduced execution time. By this way all the zero entries outside the band will not be operated on. In gaussian elimination band solving subroutine the equivalent equation to equation(3.3) is;

$$a_{ij}^* = a_{ij} - (a_{s,(i-s+1)} / a_{s1}) a_{s,(j+1-s)} \quad (3.5)$$

with the limits,

$$\begin{aligned} (s+1) &\leq i \leq (s+HBW-1) \\ 1 &\leq j \leq (HBW-(i-s)) \end{aligned}$$

where,

HBW  $\equiv$  half-bandwidth of the matrix

### 3.2.3 Square root(Cholesky) method

Another scheme which is used for the solution of the finite element method in this thesis is the square root method. A brief description of the method is presented below.

In this method the matrix [A] of the equation(3.1) is decomposed into a lower triangular matrix [L] with positive diagonal elements such that,

$$A = LL^T \quad (3.6)$$

or alternatively, A could be decomposed into an upper triangular matrix [U] satisfying,

$$A = UU^T \quad (3.7)$$

For the former decomposition, substitution of (3.5) into (3.1) results in,

$$LL^T X = B \quad (3.8)$$

Which can be written as the following sequence of equations,

$$LC = B \quad (3.9-a)$$

$$L^T X = C \quad (3.9-b)$$

$$L = \begin{bmatrix} l_{11} & \cdot & \cdot & \cdot & \cdot & \cdot & \cdot & \cdot & 0 \\ l_{21} & l_{22} & \cdot & \cdot & \cdot & \cdot & \cdot & \cdot & 0 \\ l_{31} & l_{32} & l_{33} & \cdot & \cdot & \cdot & \cdot & \cdot & 0 \\ \cdot & \cdot & \cdot & \cdot & \cdot & \cdot & \cdot & \cdot & \cdot \\ \cdot & \cdot & \cdot & \cdot & \cdot & \cdot & \cdot & \cdot & \cdot \\ \cdot & \cdot & \cdot & \cdot & \cdot & \cdot & \cdot & \cdot & \cdot \\ l_{n1} & l_{n2} & \cdot & \cdot & \cdot & \cdot & \cdot & \cdot & l_{nn} \end{bmatrix} \quad (3.10)$$

The triangular matrix  $L = [l_{ij}]$  needed in this process can be obtained explicitly from  $A = [a_{ij}]$  through the following relationships;

$$l_{ii} = (a_{ii} - \sum_{j=1}^{i-1} l_{ij}^2)^{1/2} \quad i=1, \dots, n$$

$$l_{ij} = 0 \quad i < j$$

$$l_{ij} = \frac{1}{l_{jj}} (a_{ij} - \sum_{m=1}^{j-1} l_{jm} l_{im})$$

$i = i+1, i+2, \dots, n$   
 $j = 1, 2, \dots, n$



in which summation is taken as zero if the upper limit is less than the lower limit.

This scheme is also used taking the advantage of banded character of  $[A]$  matrix. This method has no great advantages over Gauss elimination as storage is concerned. But cholesky decomposition use significantly less computation time, which is reflected in faster and cheaper solutions.

Repeating again, the two methods of solving system matrix equation described above when they are used as banded type result in quicker and cheaper solutions proportional to the bandwidth reduction.

In finite element applications, a serious problem is the inadequacy of computers in relation to the problem size. Therefore even banded type of solution methods might not be sufficient in overcoming this drawback. Some other advanced methods are devised so that the solution of finite element problems of very large size becomes possible.

### 3.3 Convergence of finite element methods

Several convergence criteria are proposed for the finite element method applications. Some of them concern the convergence of the individual steps involved in the method so to obtain more accurate results. For example if an iterative method is used for the solution of simultaneous matrix equations then the convergence of the equation solver method is looked for. But the more important form of convergence is that of the finite element method as a whole. In all such methods it is assumed that, as the numbers of elements and nodal points are increased, the resulting solution approximates more closely the true solution to the problem(2). The variational formulation described in (Appendix A) provides a general idea of the conditions required for convergence of the finite element method.

$$\chi^e = \iint \frac{1}{2} \left\{ k \left[ \left( \frac{\partial T}{\partial x} \right)^2 + \left( \frac{\partial T}{\partial y} \right)^2 \right] - qT \right\} dx dy \quad (3.11)$$

$$\chi = \sum \chi^e$$

In equation(3.11) the total value of the functional  $\chi$  of a steady state heat conduction problem is equated to the sum of the results of the relevant integrations performed over all the individual elements.

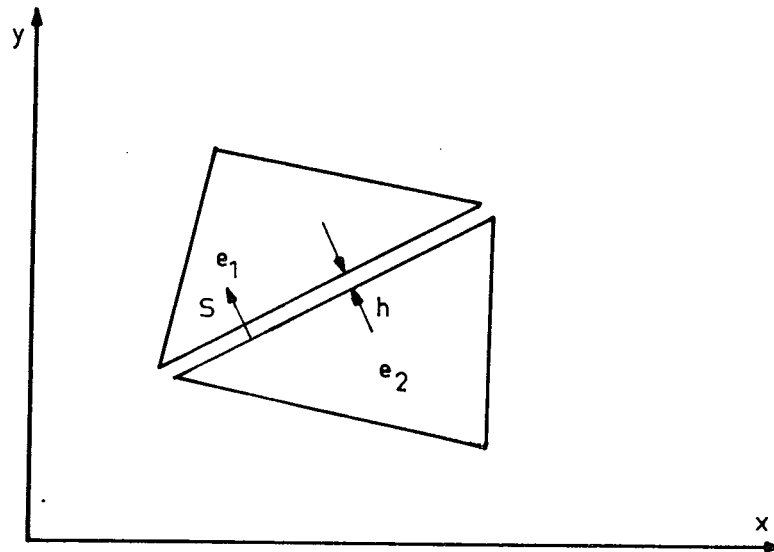


FIGURE 3.8 Two adjacent elements.

Fig.3.8 shows two adjacent elements separated along their interface by a small gap  $h$ . The condition for this interface to make no contribution to  $\chi$  is,

$$\lim_{h \rightarrow 0} \int_0^h \left[ \frac{1}{2} k \left( \frac{\partial T}{\partial x} \right)^2 + \frac{1}{2} k \left( \frac{\partial T}{\partial y} \right)^2 - qT \right] ds = 0 \quad (3.12)$$

If temperature  $T$  is continuous across the interface, its value remains constant over the gap. The first derivatives of  $T$  with respect to both  $x$  and  $y$  are therefore zero and (3.12) is satisfied.

Otherwise magnitudes of the derivatives tend to infinity as  $h$  is reduced to zero. Consequently it can be said that for this example the convergence of the whole procedure is assured if the temperature is continuous along the element interfaces.

In general terms the variational formulation provides the conditions for convergence of finite element methods. If the functional whose stationary value is sought, involves derivatives of the unknown function up to the  $n^{\text{th}}$  order, the shape functions employed within the elements should ensure continuity across element interfaces up to the  $(n-1)^{\text{th}}$  order. Elements and their associated shape functions which satisfy this requirement are said to be 'conforming' or 'compatible' (2).

#### 3.4 Truncation error

As it has already been mentioned, it is necessary to use a large number of elements and hence nodal points to achieve satisfactory convergence of the finite element problem. It is so because of the fact that the shape functions provide only approximate polynomial representations of the true variations. For instance, the temperature variation over an element given by  $T = \omega_i T_i + \omega_j T_j + \omega_m T_m$  is an approximation obtained by using shape functions  $\omega_i$ ,  $\omega_j$  and  $\omega_m$  which are first order polynomial representations derived from area coordinates.

To evaluate the truncation error involved when using finite element method, lets choose a simple example in which temperature variable is varying linearly over each element by the relationship;

$$T(x,y) = A_1 + A_2 x + A_3 y \quad (3.13)$$

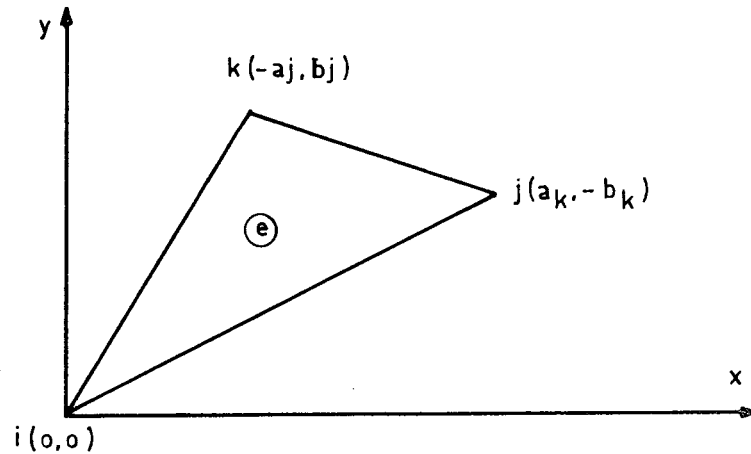


FIGURE 3.9 An element whose  $i^{\text{th}}$  node at the origin.

Suppose that the temperature variation over an element whose  $i^{\text{th}}$  node at the local origin is sought for (Fig. 3.9). The coordinates of the nodal points can be expressed in cartesian coordinates by the following terms;

$$\begin{aligned} a_i &= x_k - x_j & b_i &= y_j - y_k \\ a_j &= x_i - x_k & b_j &= y_k - y_i \\ a_k &= x_j - x_i & b_k &= y_i - y_j \end{aligned}$$

A Taylor series expansion about the origin of the local coordinates shown in Fig. 3.9 for the temperature gives,

$$T = T_i + \left( x \frac{\partial T}{\partial x} + y \frac{\partial T}{\partial y} \right) + \frac{1}{2} \left( x \frac{\partial}{\partial x} + y \frac{\partial}{\partial y} \right)^2 T + \dots \quad (3.14)$$

Using equation (3.13) and evaluating the derivatives at the origin,

$$\frac{\partial T}{\partial x} = A_2 \quad \text{and} \quad \frac{\partial T}{\partial y} = A_3 \quad \text{is obtained.}$$

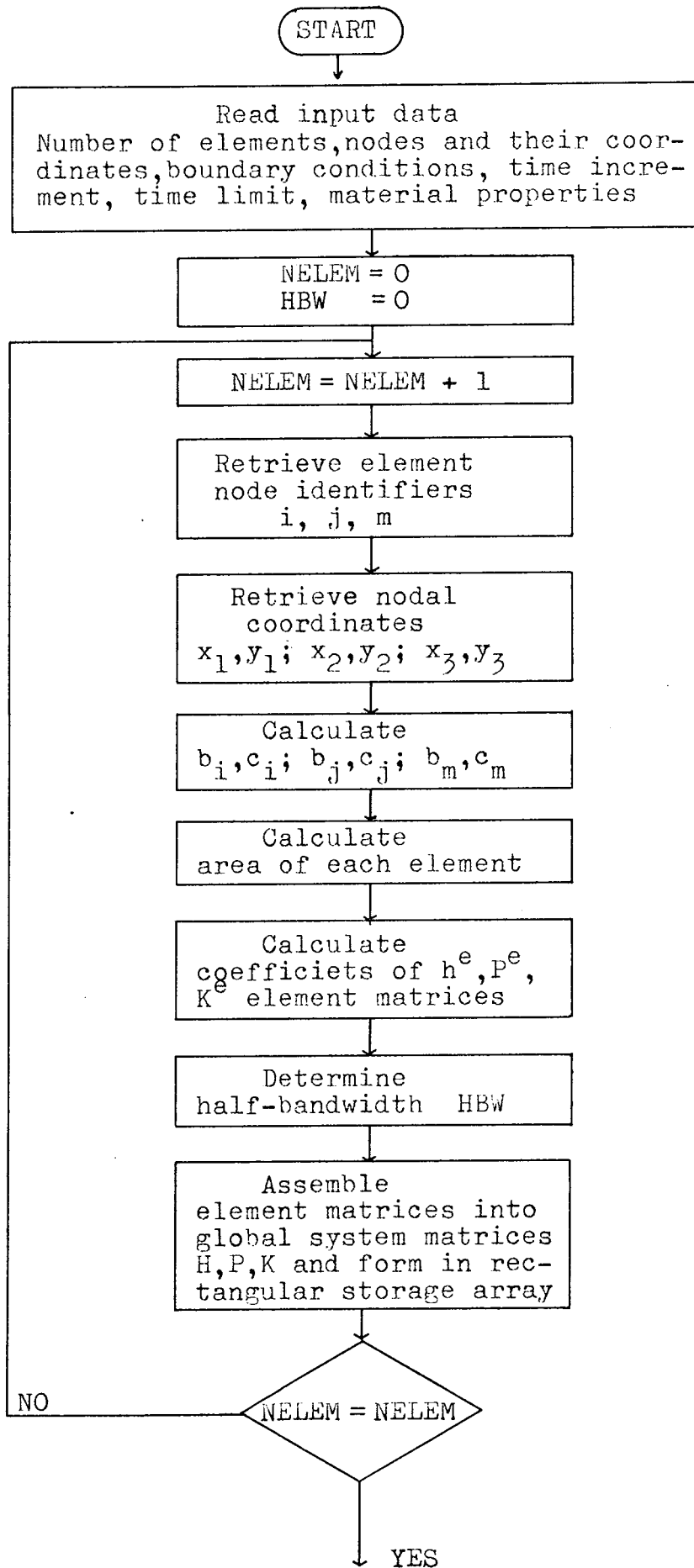
Therefore error involved in using equation(3.13) as a truncated form of equation(3.14) at point j for example is;

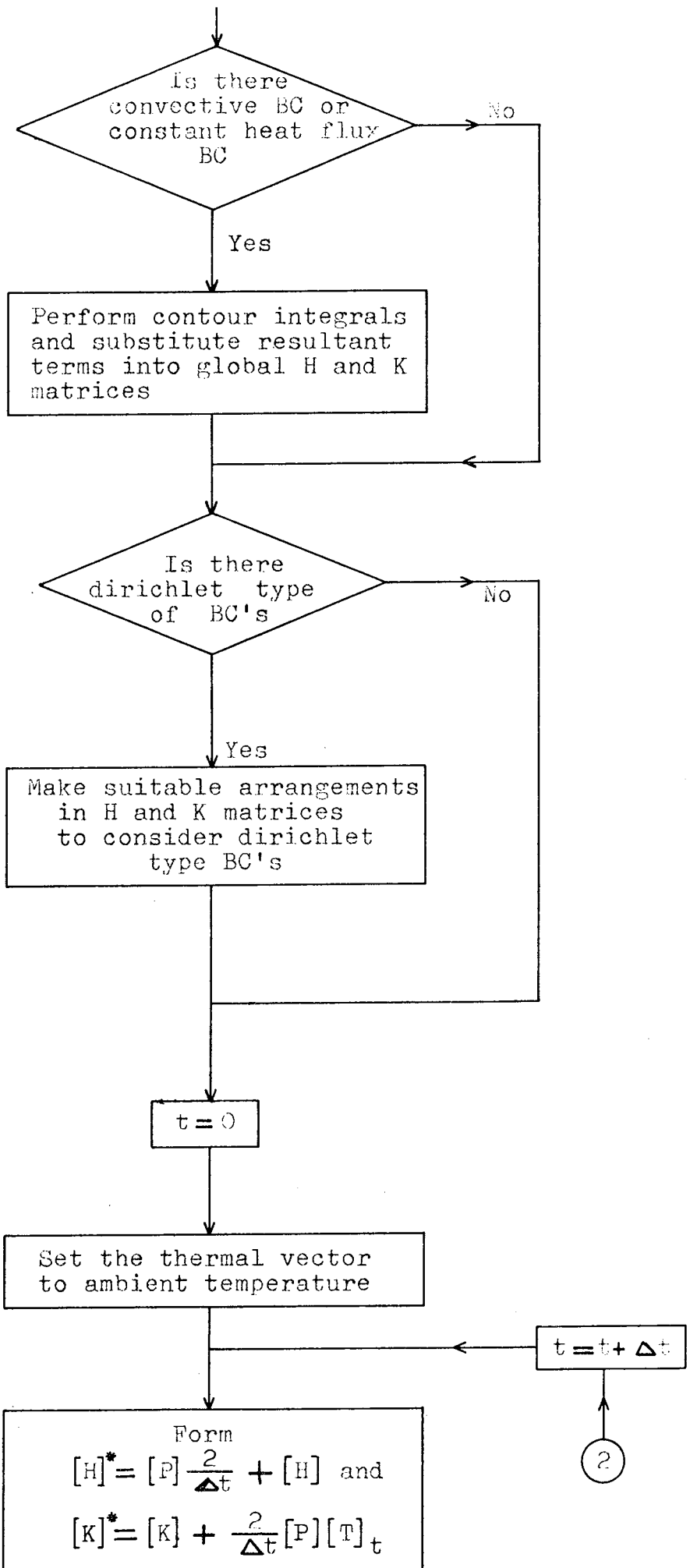
$$E_T = \frac{1}{2} \left( a_k^2 \frac{\partial^2 T}{\partial x^2} - 2a_k b_k \frac{\partial^2 T}{\partial y \partial x} + b_k^2 \frac{\partial^2 T}{\partial y^2} \right) \quad (3.15)$$

Equation(3.15) reveals that the truncation error is of the order of the square of the dimensions of the element. (i.e  $a_k, b_k \dots$  etc.) In order to minimize this error the element size must be reduced.

### 3.5 The program

A general program is developed to solve the transient thermal fields of underground cables under different conditions. For the solution of different problems only the data is needed to change. Fig.3.10 shows the flow-chart of the program.





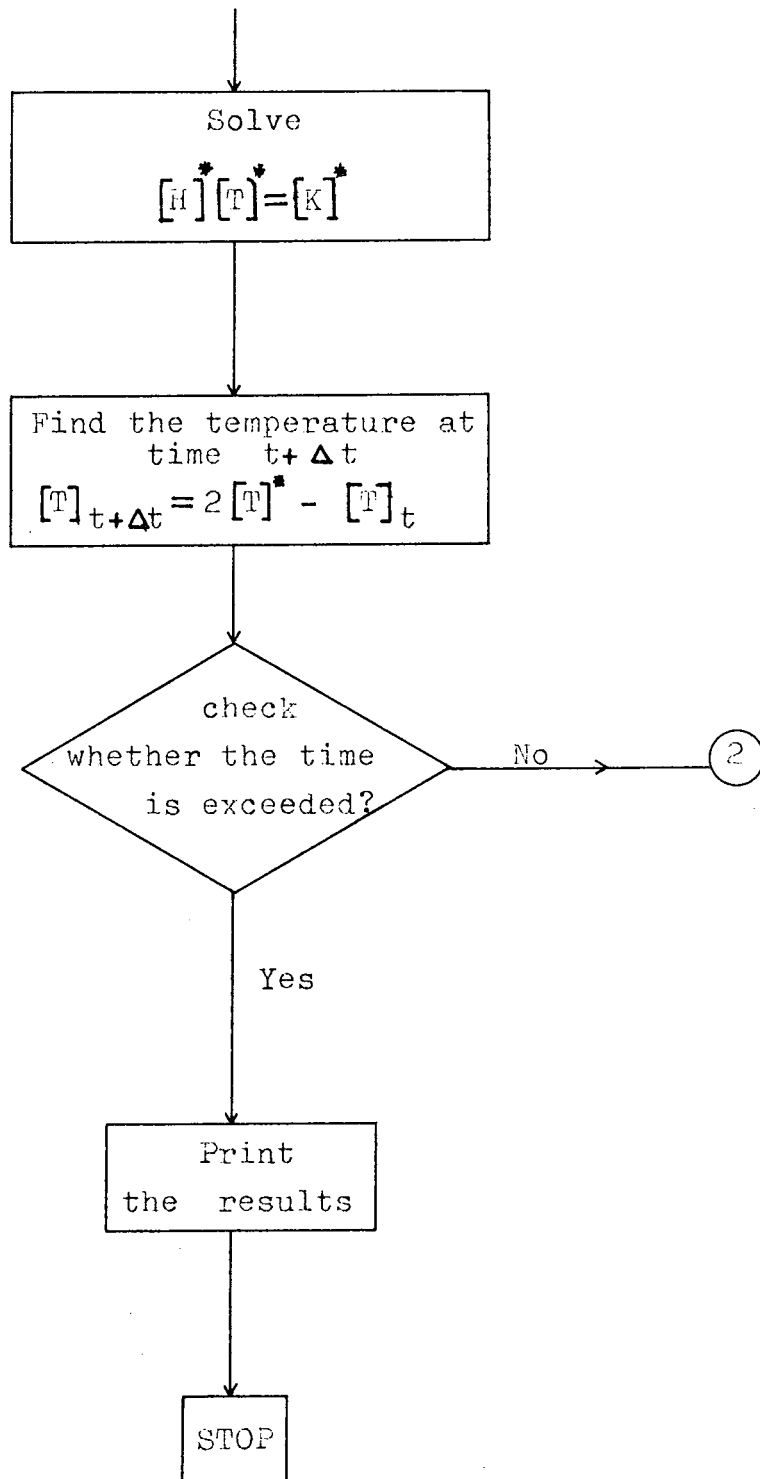


Figure 3.10 Flow-diagram of the transient thermal field program



## CHAPTER IV APPLICATIONS

### 4.1 Introduction

The demand for electric power in the highly industrialised countries has been doubling approximately every 10 years(12), and in some of the developing countries the growth rate has been even faster. For example demand growth rate for Turkey is given as 3-3.5 times for each decade(13).

With this enormous rate which is foreseen also for the coming future will necessitate a growth for power systems of greater capacities with the ability to transmit energy with very low loss over considerable distances.

Naturally, the size of the generating plant required will increase as also will the size of the generators, and it is clear that the power capability of transmission circuits will need to keep pace with the load growth. Although a major part of the increased load will still be carried by overhead lines, a consistently growing proportion of the transmission network will consist of underground power cables, since load centres nearly always coincide with densely populated urban areas. The trend towards an expansion of the underground system will certainly be reinforced by the desire to preserve the environment.

The generation and transmission of electric power is based on the fact that we have at our disposal materials such as copper and aluminium which are good conductors of electricity. The resistive nature of these materials give rise to the generation of unwanted heat which must be dissipated by the surrounding environment through electrical insulation of poor thermal conductivity. As a result, the current densities which can be obtained with copper and aluminium at ambient temperature are very low, and are of the order of  $1\text{ A mm}^{-2}$ .

This fact brings a severe limitation on the usage of underground power cables for carrying larger power capacities although the necessity of using power cables at a greater extent increases with the rapid rate of load growth all over the world.

Nowadays the techniques for increasing the power rating of cables are being improved for example artificial cooling of cables, the usage of polymeric and gas filled cables and the development in cryogenic cable technology(14).

Without going into the details of such improvements in cable technology, the fundamental factors affecting the current carrying capacities of power cables should be discussed.

The current-carrying capacity of high voltage cables is determined by the ability of the immediate environment of the cable to dissipate the heat generated within the cable.

The current-carrying capacity of cables is not dependent only on the cross-sectional area of the conductors. It is primarily a matter of heat transfer from the cable core, where the heat is mainly generated, through the cable insulation to the surrounding medium and thence finally to free air. It is therefore dependent on the various thermal conductivities of the media concerned. Especially at high voltages the voltage-dependent internal heat generation in the insulation adds to the heat produced by the conductor.

The three sources of heat generation are the resistive conductor losses, the dielectric losses and the sheath losses which for a 400KV 1935 mm<sup>2</sup> cable circuit amount in total to about 130 Wm<sup>-1</sup>(14).

In a power cable the maximum permitted insulation tempera-

ture is often a limitation to its current rating. The full utilization of the cable material is only possible if temperature can be calculated for different loading conditions.

Hereunder, some applications of the finite element method in the solution of thermal field distribution of various power cables is introduced.

#### 4.2 Simple cable problem

For most of the heat conduction problems the analytical solution is quite difficult and sometimes impossible to obtain due to the complex geometry of the solution domain. An extensive representation for analytical methods in conduction of heat in solid bodies is given in(15). These involve the derivation of the mathematical solution for the temperature as a function of space or space time coordinates. The solution must satisfy the basic governing partial differential equation, together with certain initial and boundary conditions suitable for the particular problem. But for very complex geometries and complicated boundary conditions of the physical problem concerned, the methods other than analytical ones become preferable. These can be grouped as graphical, numerical and experimental methods(16). Finite difference and finite element methods are commonly used numerical procedures in handling such problems.

In order to make a comparison between analytical and numerical methods an underground cable problem which has an analytical solution is considered. The same problem is also solved by finite difference method(17).

The problem consists of a coaxial cable with inner conductor radius  $a=0.60$  cm and the outer radius  $b=15.10$  cm. It is assumed that the conductor is insulated by homogeneous

dielectric material of thermal conductivity  
 $k=0.0022 \text{ cal. sec}^{-1}.\text{cm}^{-1}.\text{°C}^{-1}$ . A constant heat flow  
 $f_c=0.018543 \text{ cal. sec}^{-1}.\text{cm}^{-2}$  (i.e, corresponding to a cur-  
rent of 400 Amperes flowing through a conductor of 0.183 ohm/km)  
is applied from the conductor surface towards the insulation.

The cable surface ( $r=b$ ) is kept at a constant temperature  
of 25°C, then the steady-state temperature variation throughout  
the insulation is sought using transient-state thermal field  
program.

#### 4.2.1 Analytical solution

Since the steady-state results are required, the governing  
thermal field equation becomes the laplace's equation for  
which the analytical solution is given in (Appendix.C). After  
considering the boundary conditions of the constant heat  
flux and the fixed temperature on the conductor and the cable  
surfaces respectively, the exact solution takes the following  
form;

$$T(r) = 25.0 + \frac{a}{k} f_c \ln\left(\frac{b}{r}\right) \quad \text{for } a < r < b \quad (4.1)$$

#### 4.2.2 Finite element solution

Because of the symmetry, only half of the cross section  
of the cable is considered in modelling the problem(Fig.4.1).  
The region is divided into 96 elements with 63 nodal points.  
As seen in Fig.4.1 element division is indicated in one part  
of the solution region only for the demonstration of the way  
how the mesh is obtained. In solving the problem both Gaussian  
elimination and cholesky decomposition methods are used as  
simultaneous matrix equation solvers. The same routines are  
adapted to another version of storage mode, namely rectan-  
gular array storage instead of full matrix storage, which  
makes it possible to gain the benefit coming from the  
symmetrical and banded nature of the system matrices. The

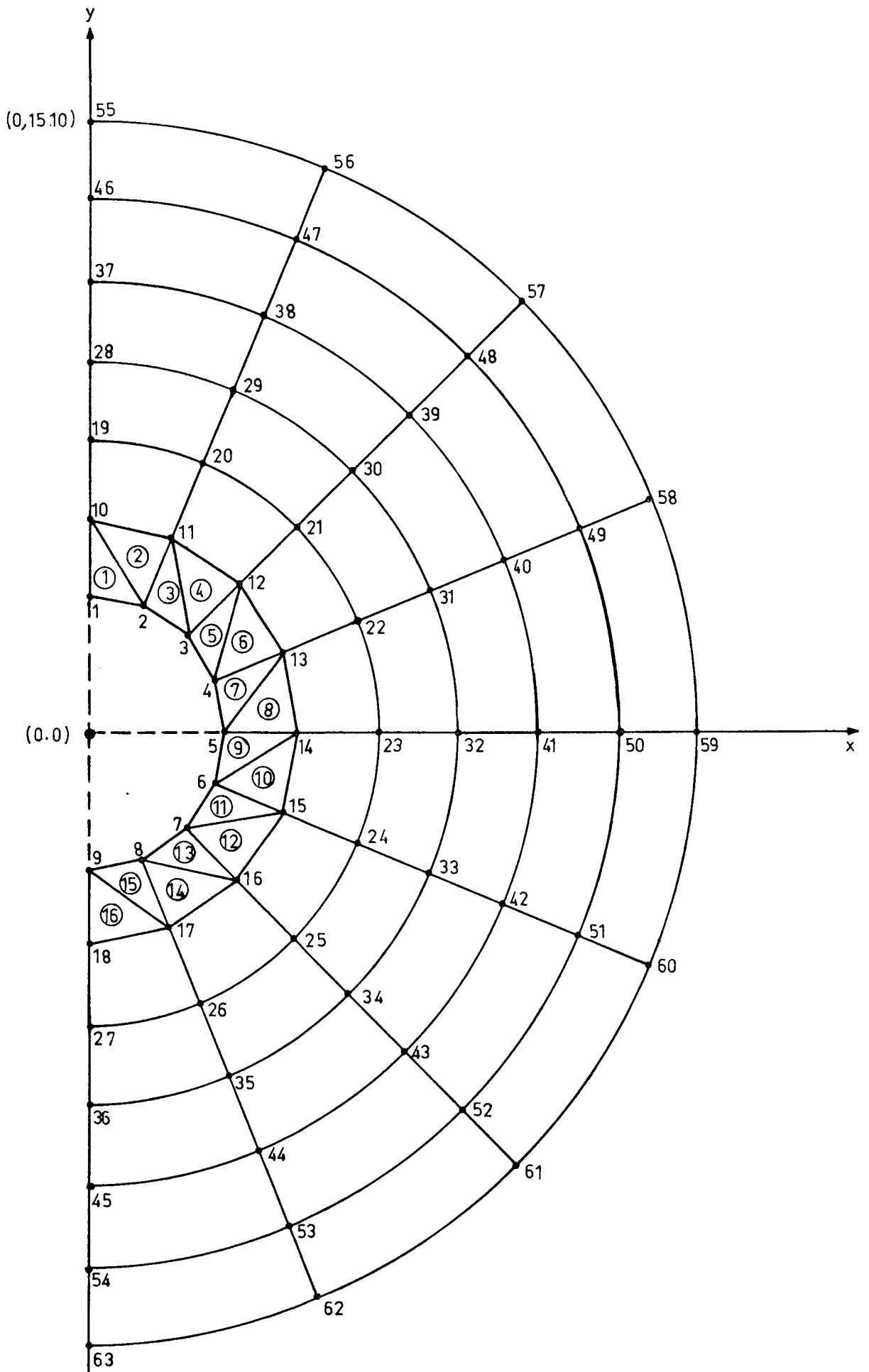


FIGURE 4.1 The geometry for simple cable problem

applications are compared in both aspects of storage requirement and execution time. Firstly the finite element mesh in Fig.4.1 is obtained by hand and the data cards; including element numbers, nodal point numbers, node identifiers corresponding to each element and also the x, y coordinates of all 63 nodal points, are prepared and given as program input. Secondly this part of the procedure is accomplished by a developed finite element mesh generation subroutine providing all geometric data of the problem automatically.

For all alternative applications the program is run for a transient temperature variation with the time limit of 250 minutes. Since the temperature variation is initially very steep, a small time increment of 15 seconds is chosen. As the time progresses, the temperature variation becomes slower and larger time increments of 30 and 60 seconds are employed in the time intervals (20 minutes, 50 minutes) and (50 minutes, 250 minutes) respectively. The programs are run with Interdata 7/32. The running times with this computer is comparatively high in comparison with more advanced machines.

When Gaussian elimination method with full matrix storage is utilized the storage requirement is 100K and the running time of the computer is about 1/2 hour. If Gaussian elimination band solver routine is used this time the storage area is reduced by  $\frac{2}{3}$  to a value of 34K with an execution time of about 8 minutes. With the usage of cholesky decomposition method banded routine required storage is 31K and the execution time is 4 minutes. Gaussian elimination band solver routine when used together with an automatic mesh generation scheme results in 41K memory space and 6 minutes of execution time. In each of these cases the compilation time is approximately seven minutes with Fortran 6 compilation. This figure is reduced below 1 minute when Fortran 7 compilation is used.

The conductor temperature and the temperature of a node in the insulation at a radial distance of 3 cm, are plotted with respect to time in Fig.4.2. The figure reveals that at the beginning both temperatures rise steeply and then as time progresses both of them converge to their steady state values.

In Fig.4.3 a radial temperature distribution at time  $t=250$  minutes is indicated. Temperature is exponentially decaying in radial direction as it is expected.

Transient results obtained using all possible schemes described above are exactly the same. Table(4.1) makes a comparison of both analytical and numerical results for different radial positions.

Node no	Radial distance (cm)	Numerical result at $t=250\text{min} (^{\circ}\text{C})$	Analytical result ( $^{\circ}\text{C}$ )
1	0.6	39.04	41.31
10	1.35	35.25	37.21
19	3	31.55	33.17
28	5	29.21	30.58
37	8	27.23	28.21
46	12	25.74	26.16
55	15.10	25.00	25.00

TABLE 4.1 Comparison of numerical and analytical results

Note that the difference between both results come from the fact that the analytical results represents steady state temperature distribution over the region concerned, while the numerical results are obtained by a transient analysis. At the end of 250 minutes largest difference between both results is only  $2^{\circ}\text{C}$ . At this instant conductor temperature reaches to  $39.04^{\circ}\text{C}$  and there is still a temperature rise of

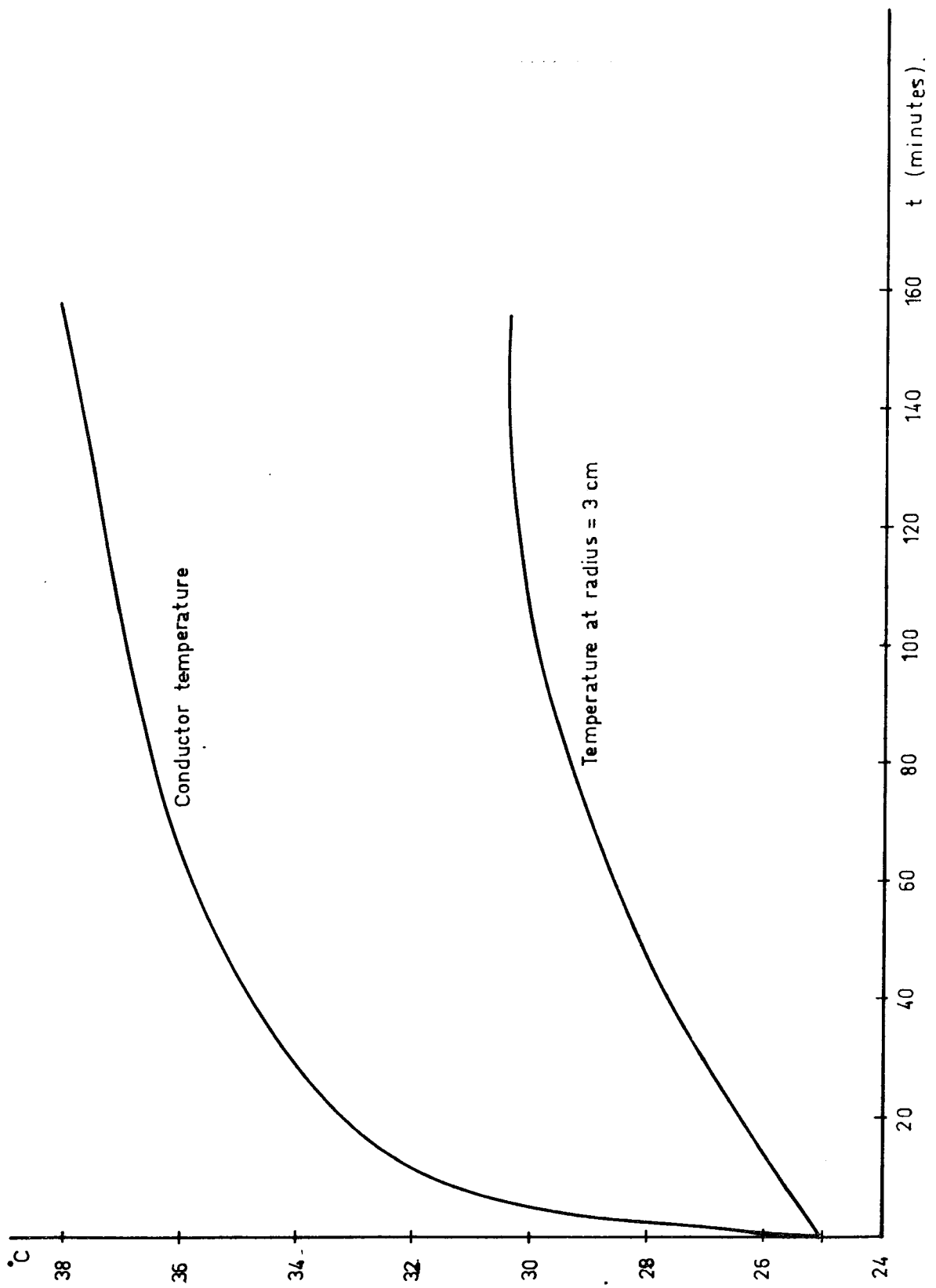


FIGURE 4.2 Variation of temperature with time.



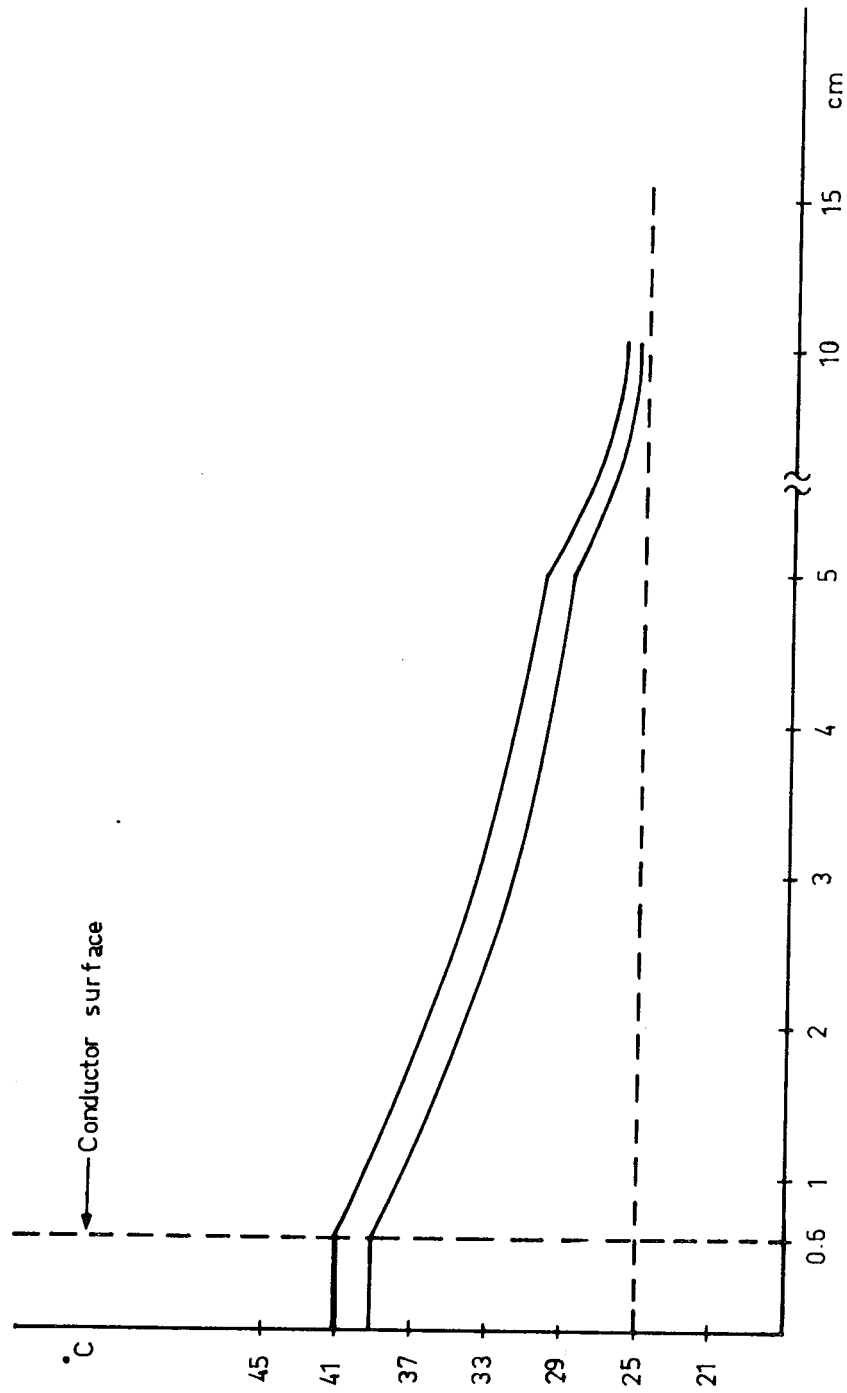


FIGURE 4.3 Temperature distribution with radius R at time  $t = 250$  minutes.

0.01°C per minute. During this time (250 minutes) most of the heat flux, from the conductor surface, is spent to heat up the cable insulation. Towards the outer surface of insulation, a larger volume has to be heated. For this reason, the temperature increase at further radial distances is very slow.

#### 4.3 Heat analysis of a 35 KV, 95 mm<sup>2</sup> cable

The maximum continuous permissible temperature of a cable determines its operation life and reliability. Overheating a cable causes a rapid ageing and deteriorates both electrical and thermal parametric values of its insulation. As it is mentioned previously, heat generation in a cable, is caused by the heat dissipation in the cable core and the dielectric losses within the insulation.

In this section, a transient heat analysis is carried out for a 35 KV Siemens 95 mm<sup>2</sup> single core cable which is manufactured and utilized in Turkey, and the results are discussed in various aspects.

##### 4.3.1 Modelling of the problem

Although the power cables are generally buried at a depth of about 60 cm in practice, the cable in this analysis is considered to lie at a depth of 15.30 cm, since the thermal distribution throughout the soil does not change too much after such a distance away from the cable. The modelling of the problem for the thermal analysis is indicated in Fig.4.4. Assuming symmetry only the half of the region is considered. The cable cross section and the surrounding soil are divided into appropriate triangular elements. As Fig.4.4 clearly reveals that the cable cross section is divided into elements such that the conductor and insulation circular boundaries are replaced by polygonal boundaries. This introduces a small error in the representation of the

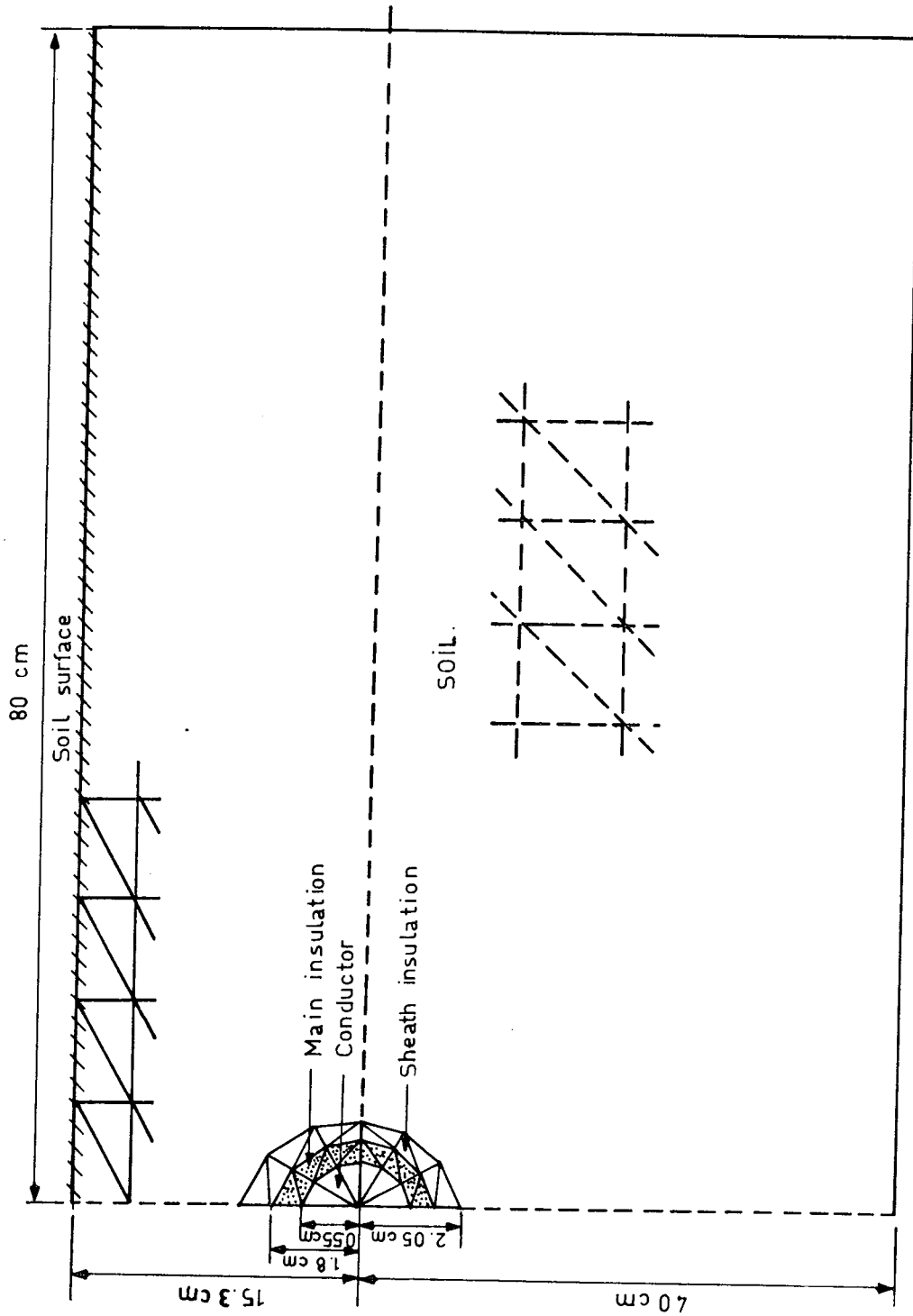


FIGURE 4.4 35 KV Single cable installation and element division.

cable. The resultant number of elements and nodal points are 116 and 75 respectively. In the region close to the cable position, the elements are chosen as sufficiently small in dimension, whereas at further distances larger elements are utilised for accuracy purposes.

Heat generation is considered to be caused by the heat dissipation in the cable conductor and the dielectric losses throughout the insulation.

Since the sheath of the cable is grounded from both ends, the electric field and hence the dielectric losses are considered only throughout the main insulation and not sheath insulation.

The boundary conditions are set as follows. All the heat generated in the cable is leaving the region through the soil surface where convective boundary condition is applied. The air temperature is set equal to 25°C. The other boundary surfaces are considered non conducting meaning that the normal gradient  $\frac{\partial T}{\partial n}$  is equal to zero at these boundary surfaces.

Properties of the cable and the surrounding medium is given in Table(4.2)

PROPERTIES OF THE CABLE

Rated voltage	: 35 KV
Rated current	: 335 A
Permissible temperature	: 90°C
Dielectric constant of insulation( $\epsilon$ )	: $2.3 \epsilon_0$
Thermal conductivity of insulation(k)	: $0.0008 \text{ cal. sec}^{-1} \cdot \text{cm}^{-1} \cdot \text{°C}^{-1}$
Specific heat capacity of insulation(c)	: $0.55 \text{ cal. gr}^{-1} \cdot \text{°C}^{-1}$
Density of insulation( $\rho$ )	: $0.94 \text{ gr. cm}^{-3}$
Conductor resistance	: $0.188 \text{ ohm. km}^{-1}$
Sheath resistance	: $1.116 \text{ ohm. km}^{-1}$
Temperature coefficient( $\theta$ )	: $0.00393 \text{ °C}^{-1}$
Cable radius	: 2.05 cm
Core insulation thickness	: 1.25 cm
Sheath insulation thickness	: 0.25 cm
Conductor radius	: 0.55 cm

PROPERTIES OF SOIL AND AIR

Thermal conductivity of soil(k)	: $0.00058 \text{ cal. sec}^{-1} \cdot \text{cm}^{-1} \cdot \text{°C}^{-1}$
Specific heat capacity of soil(c)	: $0.20 \text{ cal. gr}^{-1} \cdot \text{°C}^{-1}$
Density of soil( $\rho$ )	: $1.20 \text{ gr. cm}^{-3}$
Heat transfer coefficient for still air:	$0.000125 \text{ cal. cm}^{-2} \cdot \text{sec}^{-1} \cdot \text{°C}^{-1}$

TABLE 4.2 Properties of 35 KV Siemens 95 mm<sup>2</sup> single core cable, soil and air.

#### 4.3.2 Program and the discussion of results

Transient thermal behaviour of the cable and the environment is computed by the developed finite element program for different load currents of 200, 250, 300, 350, 400 A's. The ohmic resistance of the cable conductor and the dielectric loss throughout the main insulation is considered to be temperature independent for each loading condition. The data for the resistance of the conductor, heat generation in cable core and the heat generation in the main insulation for different load currents are calculated in accordance with section 2.1.1 and listed in Table(4.3). In calculating the conductor resistance a reasonable temperature value (indicated in paranthesis in Table 4.3.) is chosen and the resistance found in this way is taken to be constant throughout the transient period.

Load current (A)	Conductor resistance $10^{-5}$ ohm/cm	Heat generation in core ( cal/sec.cm <sup>3</sup> )	Heat generation in dielectric ( cal/sec.cm <sup>3</sup> )
200	0.199(35°C)	0.020	$2 \times 10^{-5}$
250	0.206(45°C)	0.032	"
300	0.212(52.5°C)	0.048	"
350	0.221(65°C)	0.068	"
400	0.232(80°C)	0.093	"

TABLE 4.3 Data for conductor resistance and heat sources.

Heat generation in the dielectric is comparatively low at this voltage level as revealed by the Table(4.3). So it can be said that the electrical stress on the insulation causes almost a negligible effect on the heating of the cable. This result, of course, arise from the fact that the polyethylene insulation has a low dielectric constant compared with other insulating materials.

Initially, temperatures of all nodes are taken as  $25^{\circ}\text{C}$ . A small time increment of 15 seconds is used at the beginning and after certain periods larger time increments of 30 and 60 seconds are applied. These larger time increments taken at the further steps of the analysis provides a considerable saving in computer time coming from the number of iterations. For each of the load current transient analysis is realised for 6 hours and the transient behaviour of both the conductor and the cable surface in this time interval are plotted in from Fig.4.5. to 4.9.

It can be observed that the conductor temperatures rise sharply at the initial times of the transient analysis (first 15-20 minutes) and thereafter the rate of rise of the temperature decreases as time progresses, consequently the temperature may be assumed to attain its steady state value as more time elapses. Indeed, for each case, the temperature increase at the end of 6 hour is comparatively low. For example for 200A load current, in the first 20 minutes the temperature rise of  $0.2^{\circ}\text{C}/\text{minute}$  is observed. However the temperature rise within the 6<sup>th</sup> hour is just  $0.007^{\circ}\text{C}/\text{minute}$ . The same figures obtained for 400A current are  $9.5^{\circ}\text{C}/\text{minute}$  and  $0.035^{\circ}\text{C}/\text{minute}$  respectively.

When cable is loaded with 400A current, at the end of 6 hour, cable core temperature reaches to  $78^{\circ}\text{C}$  as shown in Fig.4.9. Since maximum permissible temperature value for polyhethylene insulation is given as  $90^{\circ}\text{C}$  at steady state operating conditions it can be concluded that it will be dangerous for the insulation to load the cable for current values higher than 400A. This current value is higher than the 335A current value, which is given by Siemens company as rated current for  $95\text{ mm}^2$  power cables(18)

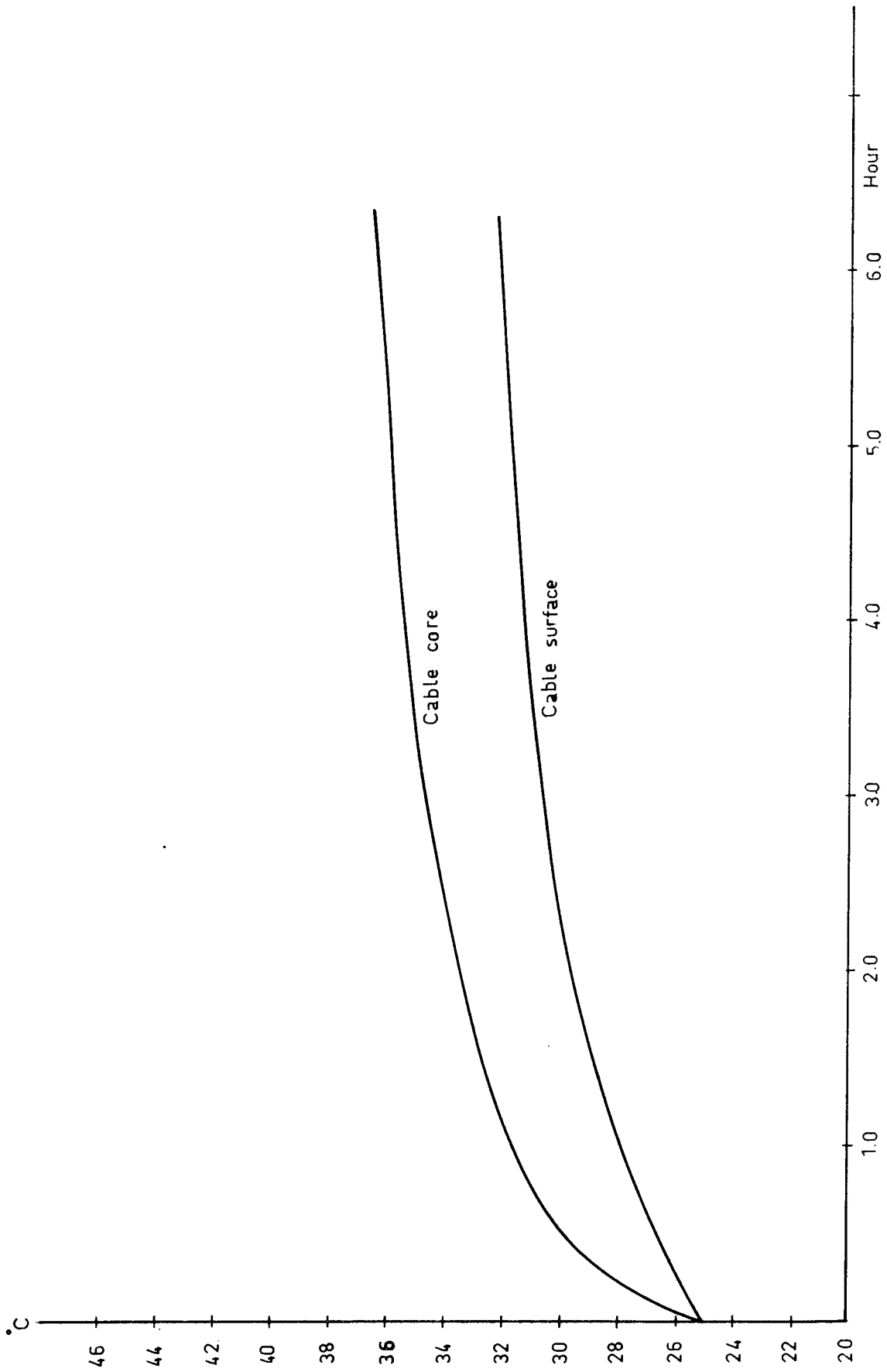


FIGURE 4.5 Cable core and cable surface temperature variation v.s. time (for 200 A core current).



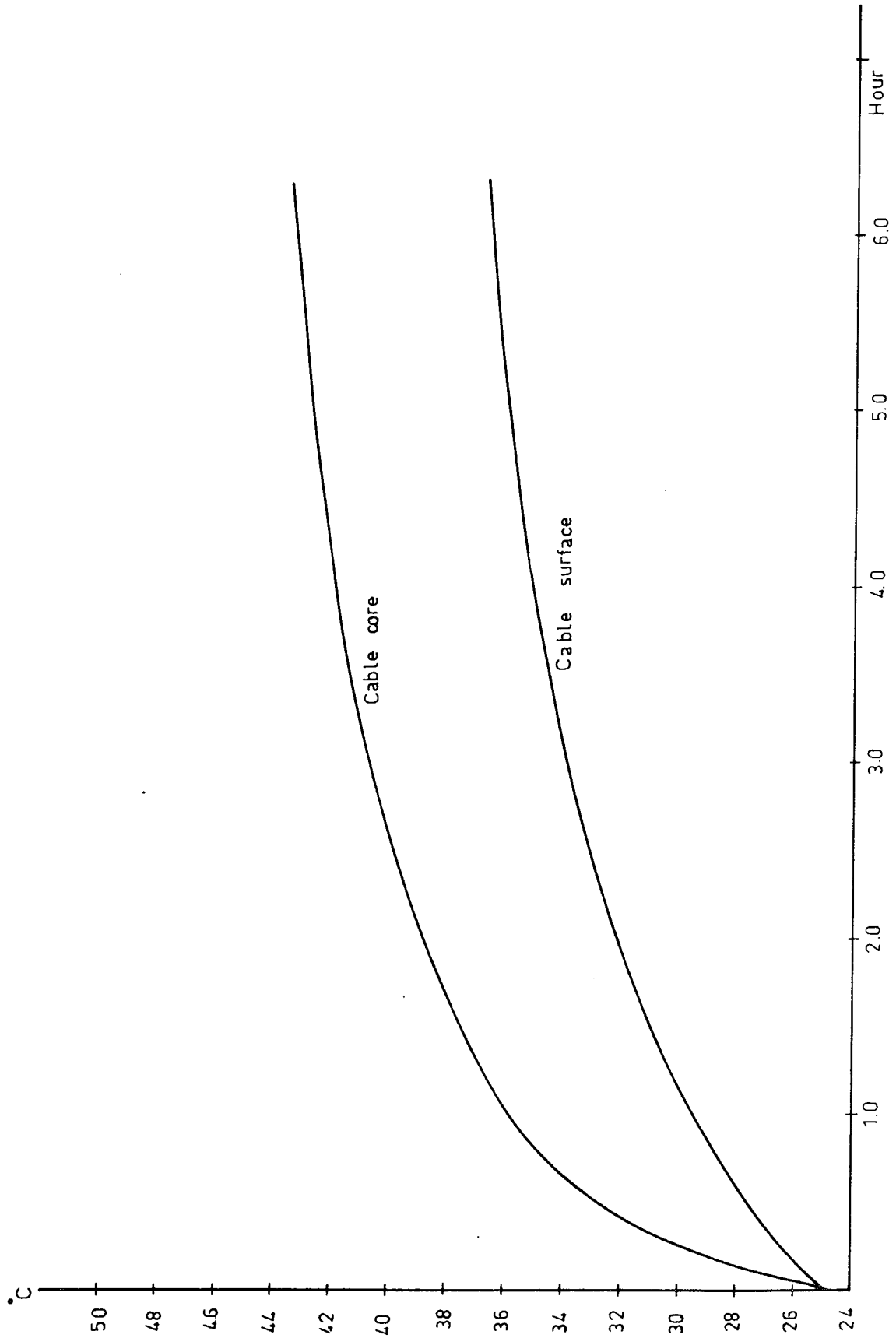


FIGURE 4.6 Cable core and cable surface temperature variation v.s. time (for 250 A core current)

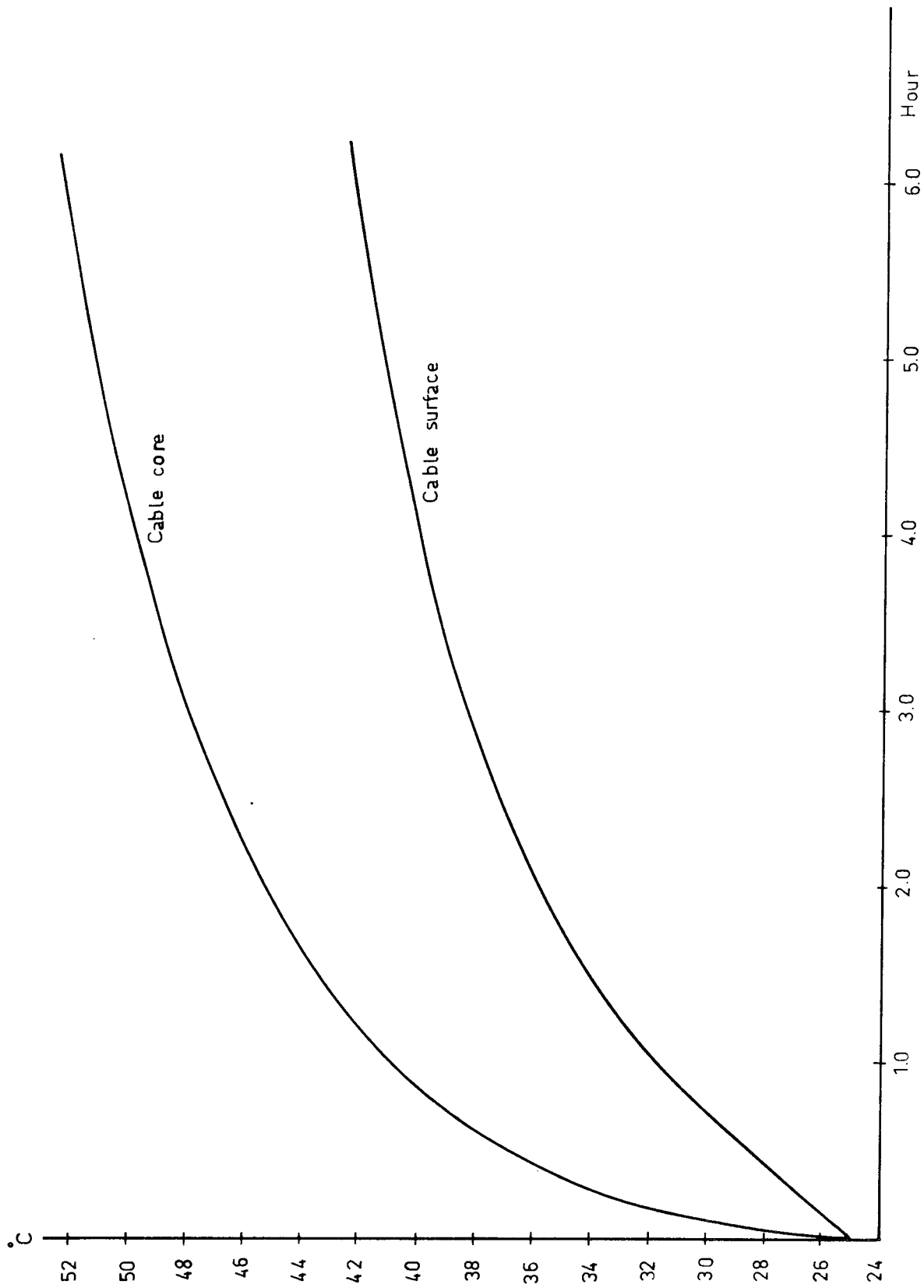


FIGURE 4.7 Cable core and cable surface temperature variation vs.time (for 300 A core current).

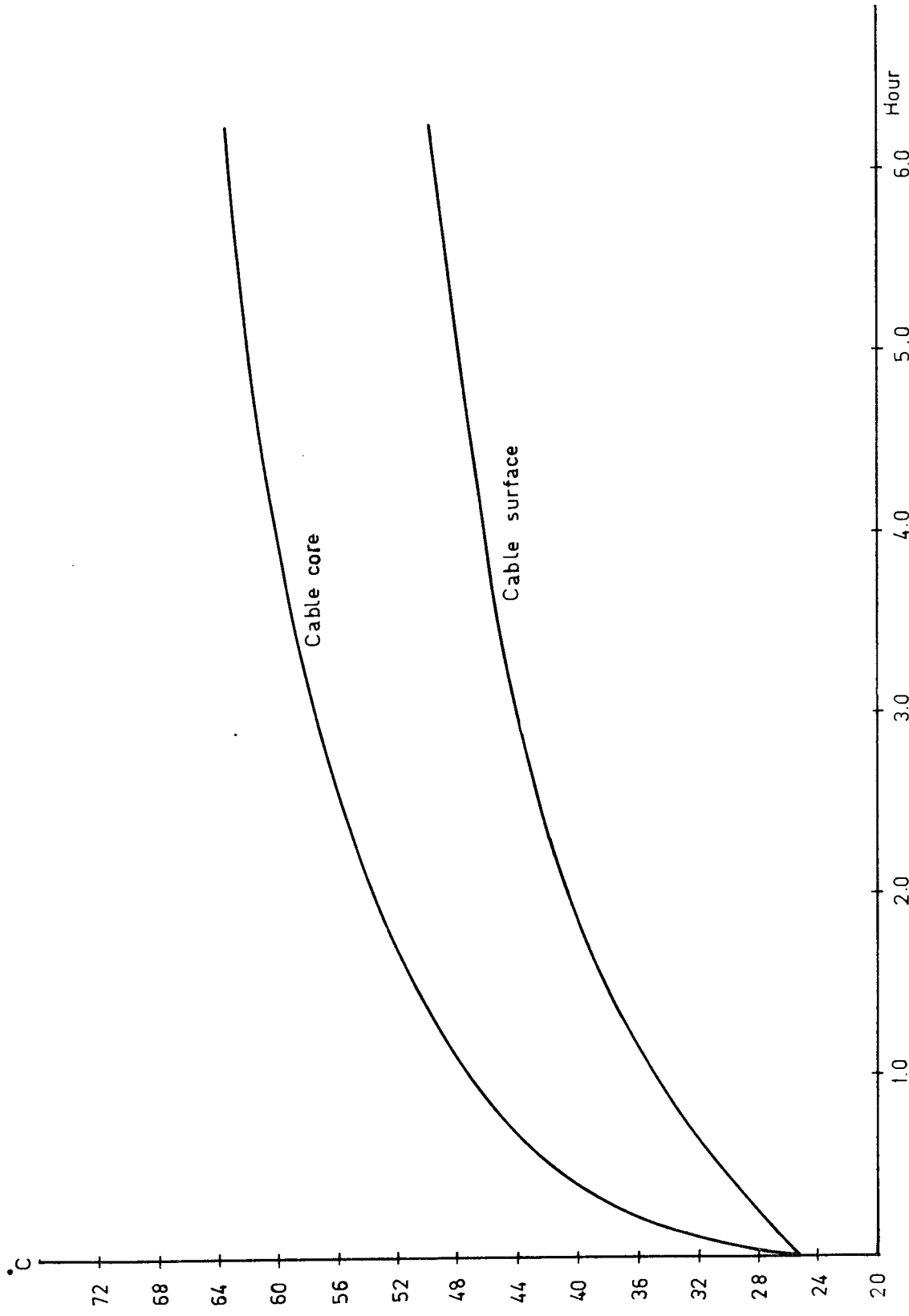


FIGURE 4.8 Cable core and cable surface temperature variation v.s. time (for 350 A core current)

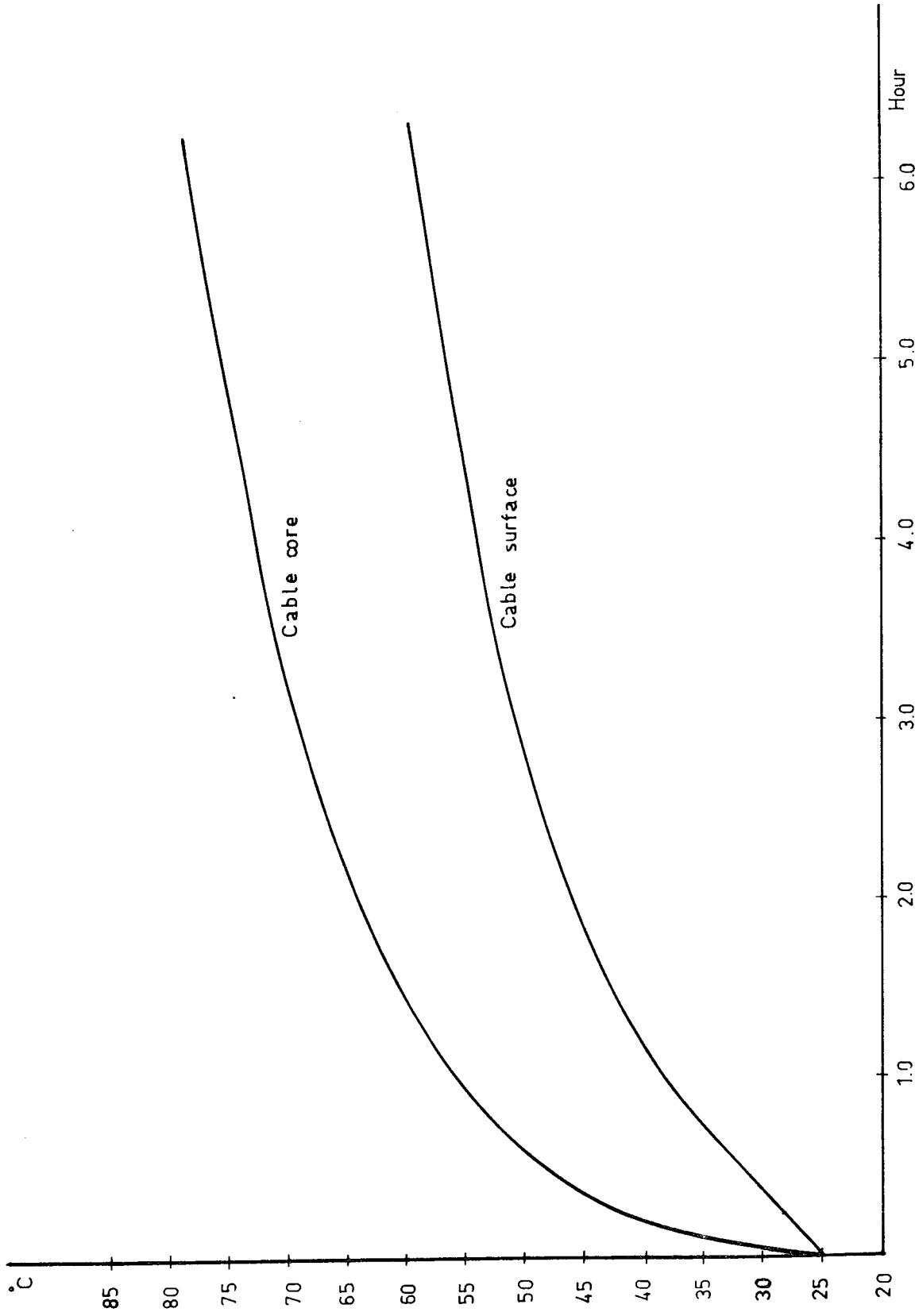


FIGURE 4.9 Cable core and cable surface temperature variation vs. time (for 400 A core current).

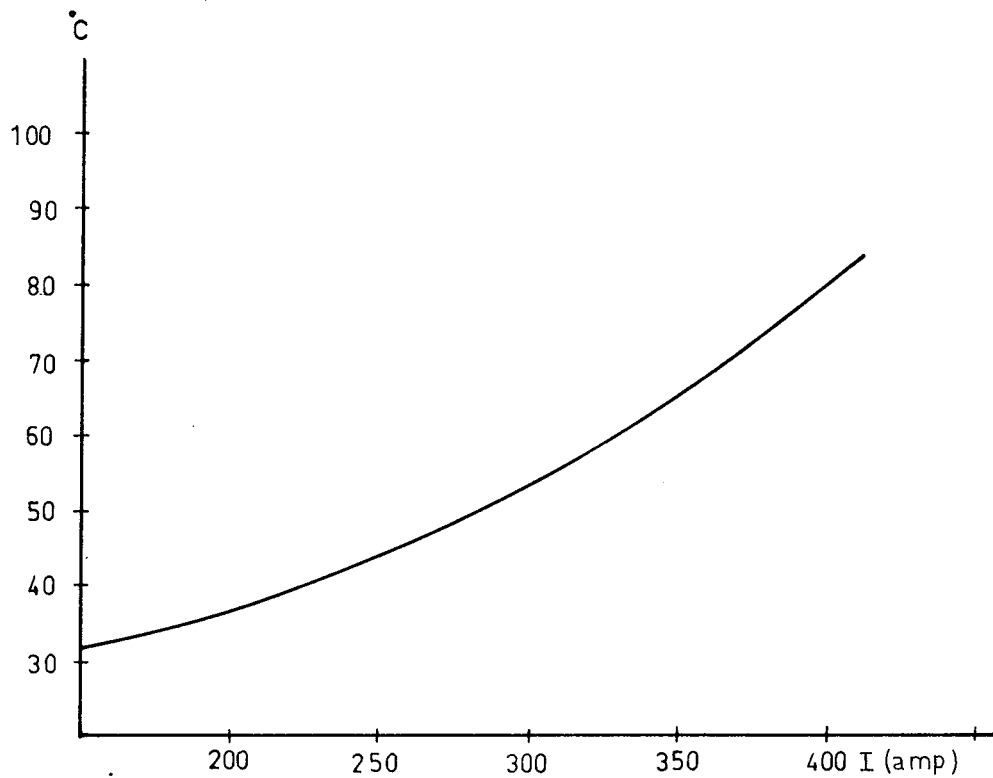


FIGURE 4.10 Steady state cable core temperature vs. current.

Fig.4.10 is a plot of steady state core temperatures obtained for different load currents. This plot reveals that the steady state core temperatures vary in a parabolic nature with different core currents. This result is expected because of the fact that the main source of heat generation is  $I^2R$  losses in the conductor and the steady state temperatures of cable conductor change in a second order proportion with the load current.

Temperature distributions (at the end of 6 hour) in the cable and the environment are plotted in Fig.4.11 and 4.12 for 250A and 350A load currents. Temperature variation with the distance from the plane of symmetry for 15.3 cm depth below

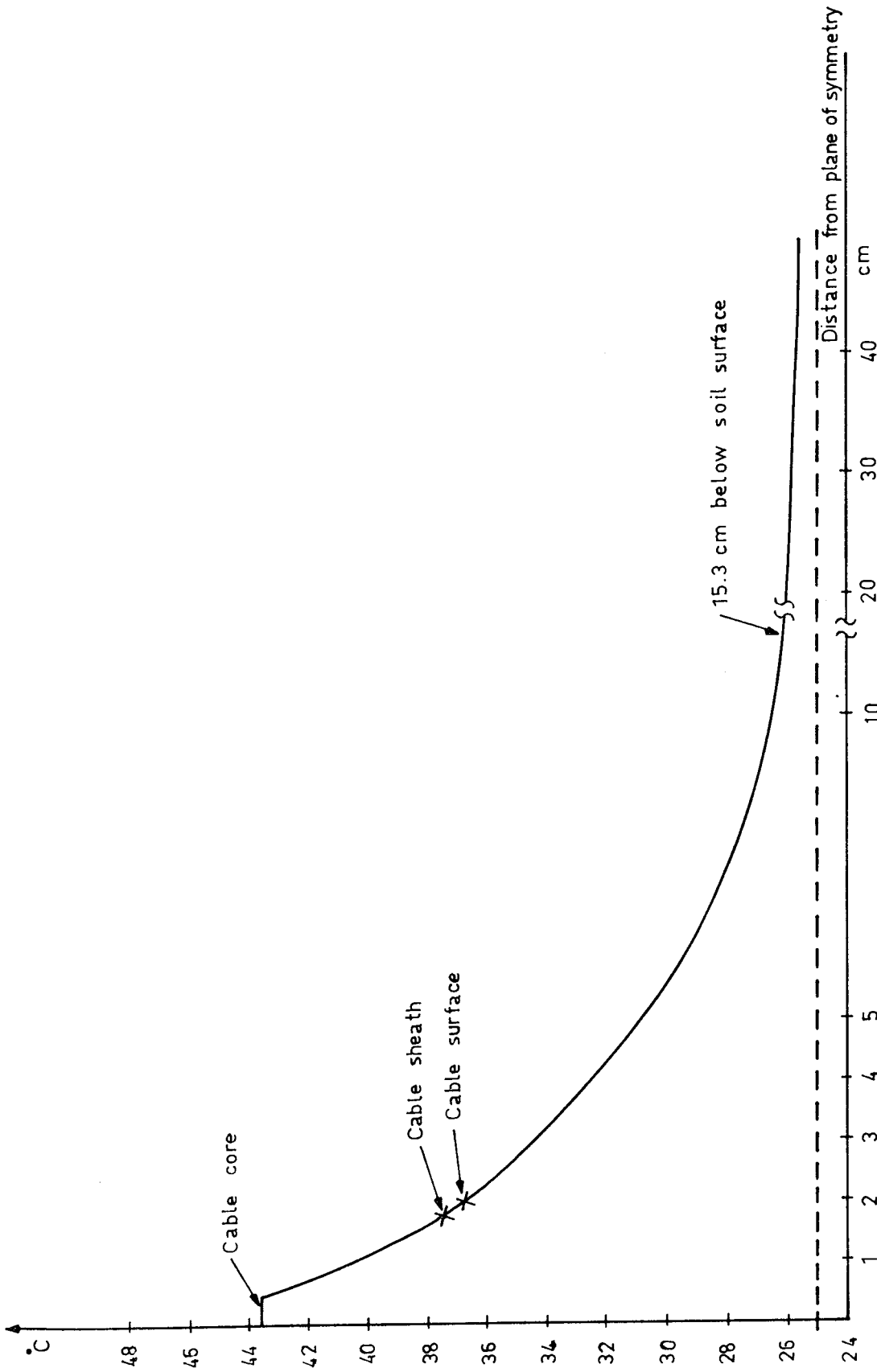


FIGURE 4.11 Temperature distribution of 35 KV cable carrying 250 A current (at time 6 hour).

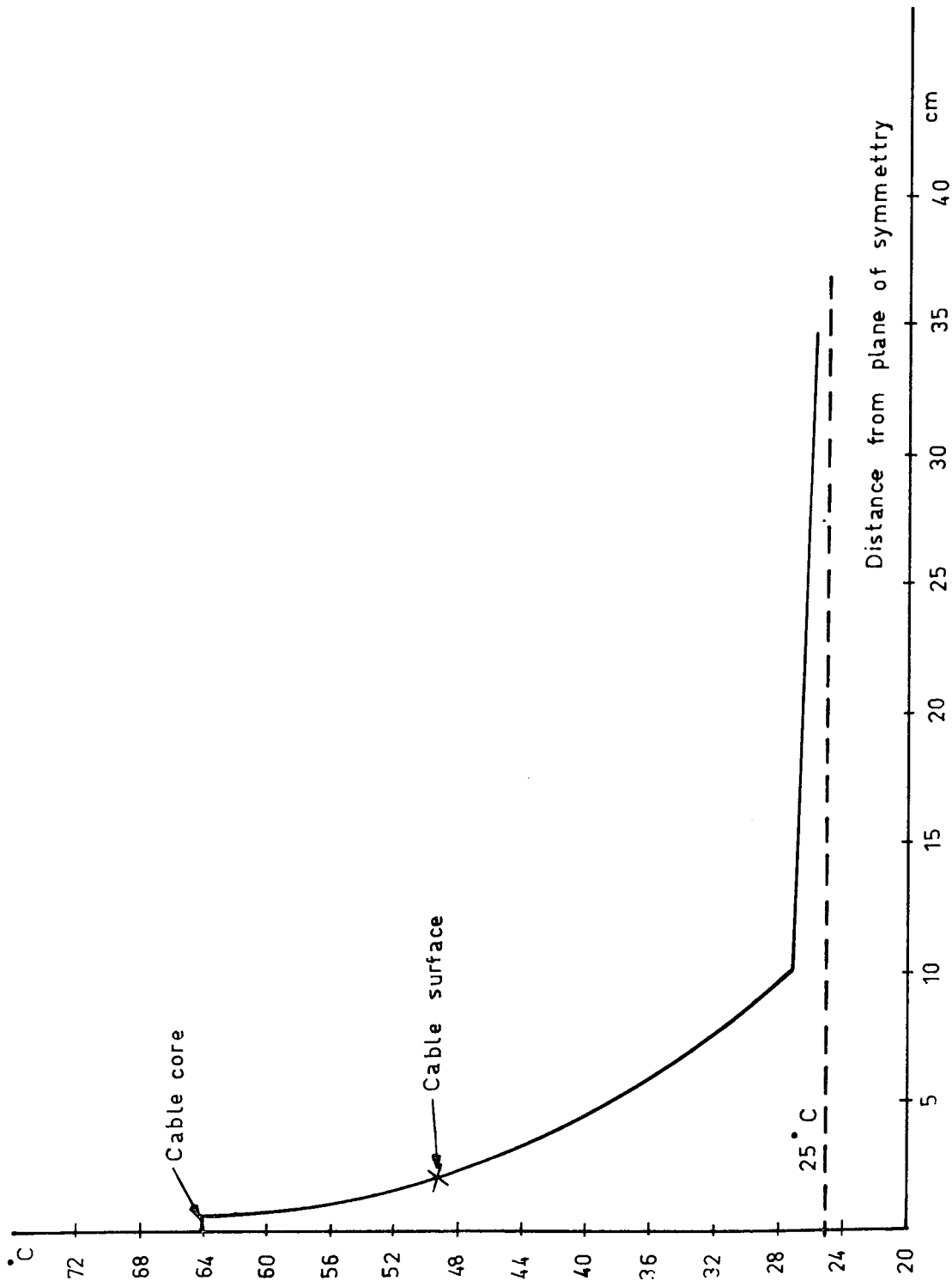


FIGURE 4.12 Temperature distribution of 35 KV cable carrying 350 A current (At time 6 hour).

soil surface is plotted. From Fig.4.11 it can be observed that the highest temperature is inside the core computed as  $43.5^{\circ}\text{C}$ , and the sheath and cables surface temperatures are  $37.5^{\circ}\text{C}$  and  $36.8^{\circ}\text{C}$  respectively. As we go further away from the symmetry plane temperature in the surrounding medium decreases exponentially and converges nearly to  $25^{\circ}\text{C}$ .

The same analysis is previously done by finite difference method and also experimental results are available(19).

A comparison of all these results reveals that there are no sounding differences between each of them. In some loading conditions there appears some little differences in the order of a few degrees which might arise from the fact that the initial conditions are selected as  $25^{\circ}\text{C}$  in finite element program where as in experimental work this value differs for each case depending upon the ambient conditions. Another possible source of error with the finite element program comes from the consideration that the conductor resistance is taken as a temperature independent element.

Finally, considerin Fig.4.10 again, it can be said that the cable can be safely loaded up to 350A which is above its rated value of 335A. Here, taking into account the given maximum permissible temperature for polyethylene insulation for continuous operation, a safety interval of temperature is considered.

#### 4.4 Heat analysis of a three phase 275KV cable

The temperature transients in a 275KV oil/paper insulated three buried power cable system is calculated when the load current has a specified variation with time. The problem and all the relevant data are taken from N.Flatabo(20).



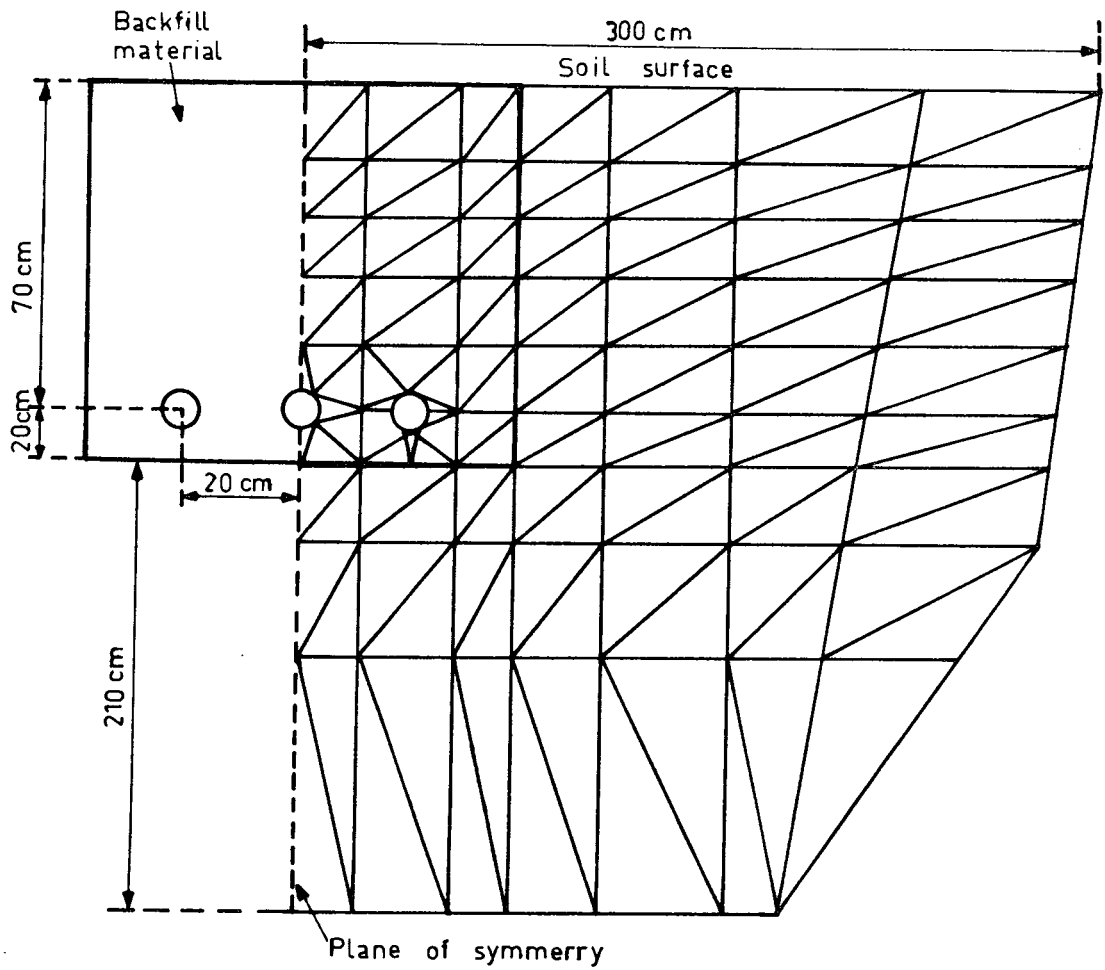
#### 4.4.1 Modelling

The three cables are placed horizontally at 70 cm depth, with 20 cm centerspace, as shown in Fig.4.13. The cable cross section and the surrounding soil are divided into triangular elements. Total number of elements and nodal points are 160 and 98 respectively. Assuming symmetry, only half of the region is divided into elements as shown in Fig.4.13.

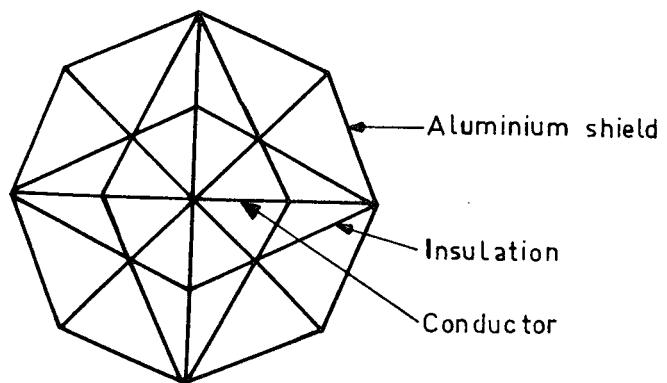
Boundary conditions are taken as follows. At the soil surface a convective boundary condition is considered. There are 8 elements next to the soil surface, for which convective boundary condition is applied at their sides. A constant heat flux boundary condition is applied for each of the cable boundary, evolving from the assumption that some amount of power loss takes place in the cable aluminium shield. This shield loss for middle cable is set equal to 25 percent of the power loss in the conductor. The shield loss is taken 7 percent of the conductor loss for the outer cables. There are 12 each such element sides constituting the cable shield boundaries, at which this type of boundary condition is considered. The other boundary surfaces are considered non conducting, i.e the normal gradient  $\frac{\partial T}{\partial n}$  is equal to zero at these boundary surfaces.

Main heat generation occurs in the cable conductor and in the cable insulation.  $I^2R$  losses and dielectric losses (3.5 W/m for each phase) are calculated as stated in chapter II.

The data associated with the cable and the surrounding soil is listed in Table(4.4)



-275 KV 3 $\phi$  Cable installation and triangular elements.



- Cable cross section divided into triangular elements.

FIGURE.4.13 A three phase 275 KV cable layout

Rated voltage	: 275KV
Material of the insulation	: oil/paper
Material of cable conductor	: copper
Dielectric constant of insulation	: 3.5
Thermal conductivity of insulation	: 0.2 W/m <sup>0</sup> C
Heat capacity of insulation	: 1.6x10 <sup>6</sup> J/m <sup>3</sup> °C
Thermal conductivity of conductor	: 372 W/m <sup>0</sup> C
Heat capacity of conductor	: 3.46x10 <sup>6</sup> J/m <sup>3</sup> °C
Conductor radius	: 1 cm
Thickness of insulation	: 2 cm
Thickness of aluminium shield	: 0.2 cm
Overall diameter of the cable	: 6.4 cm
The dielectric loss in each phase	: 3.5 W/m
Thermal conductivity of backfill material	: 0.8 W/m <sup>0</sup> C
Heat capacity of backfill material	: 2x10 <sup>6</sup> J/m <sup>3</sup> °C
Thermal conductivity of soil	: 1 W/m <sup>0</sup> C
Heat capacity of soil	: 2x10 <sup>6</sup> J/m <sup>3</sup> °C
Heat transfer coefficient	: 5 W/m <sup>2</sup> °C
The air temperature	: 15°C

TABLE 4.4 Data for the 275KV cable and the environment.

#### 4.4.2 Results and discussions

Temperature transients of the three phase cable is obtained when the load current has a prescribed variation with time as indicated in Fig.4.14.

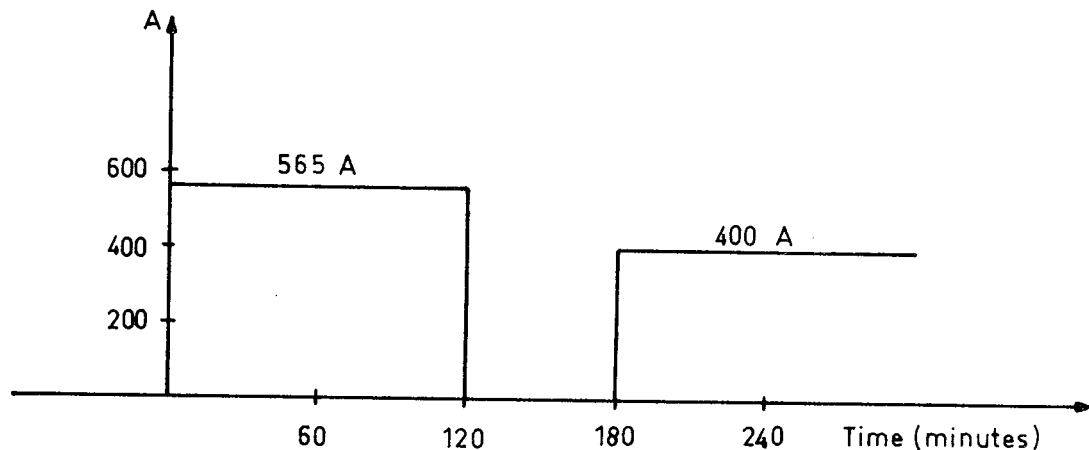


FIGURE 4.14 Load current

The temperature distribution at time  $t=0$  is the steady state temperature distribution corresponding to a load current of 400A. Steady state conditions are assumed to be attained after running the transient program for a sufficient time with the cable is loaded with 400A current. At time  $t=0$ , the load current is increased to 565A, which means that the power loss in each conductor doubles. For the period when the load current is zero, the system voltage is also assumed to be switched off, implying that both sources of heat generation, namely, power losses and dielectric losses are zero. After time  $t=180$  minutes the cable is again loaded with 400A current. Fig.4.15 shows the temperature variation at various parts of the region when the cyclic load represented by Fig.4.14 is applied.

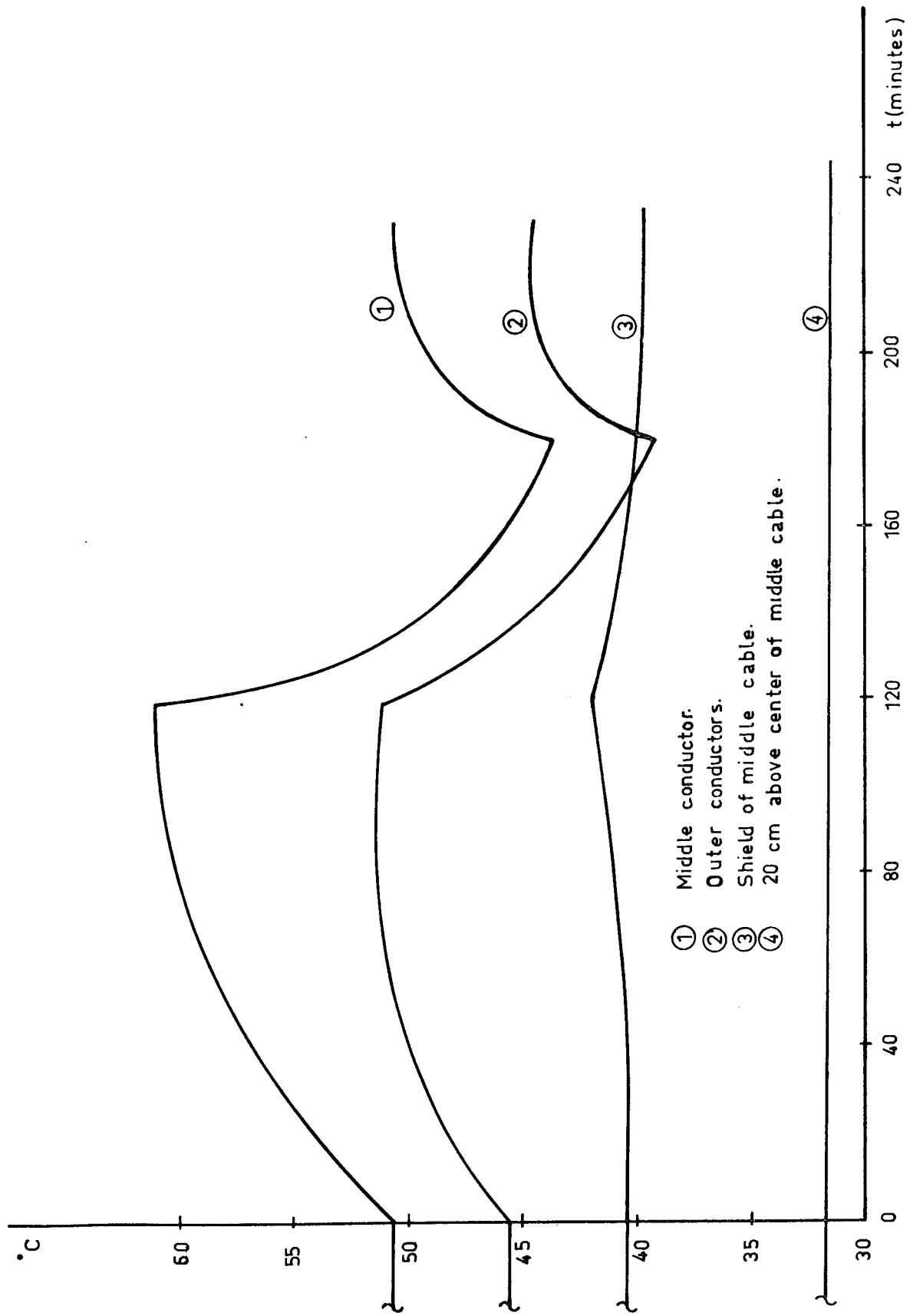


FIGURE 4.15 Transient temperatures in 275 KV cable

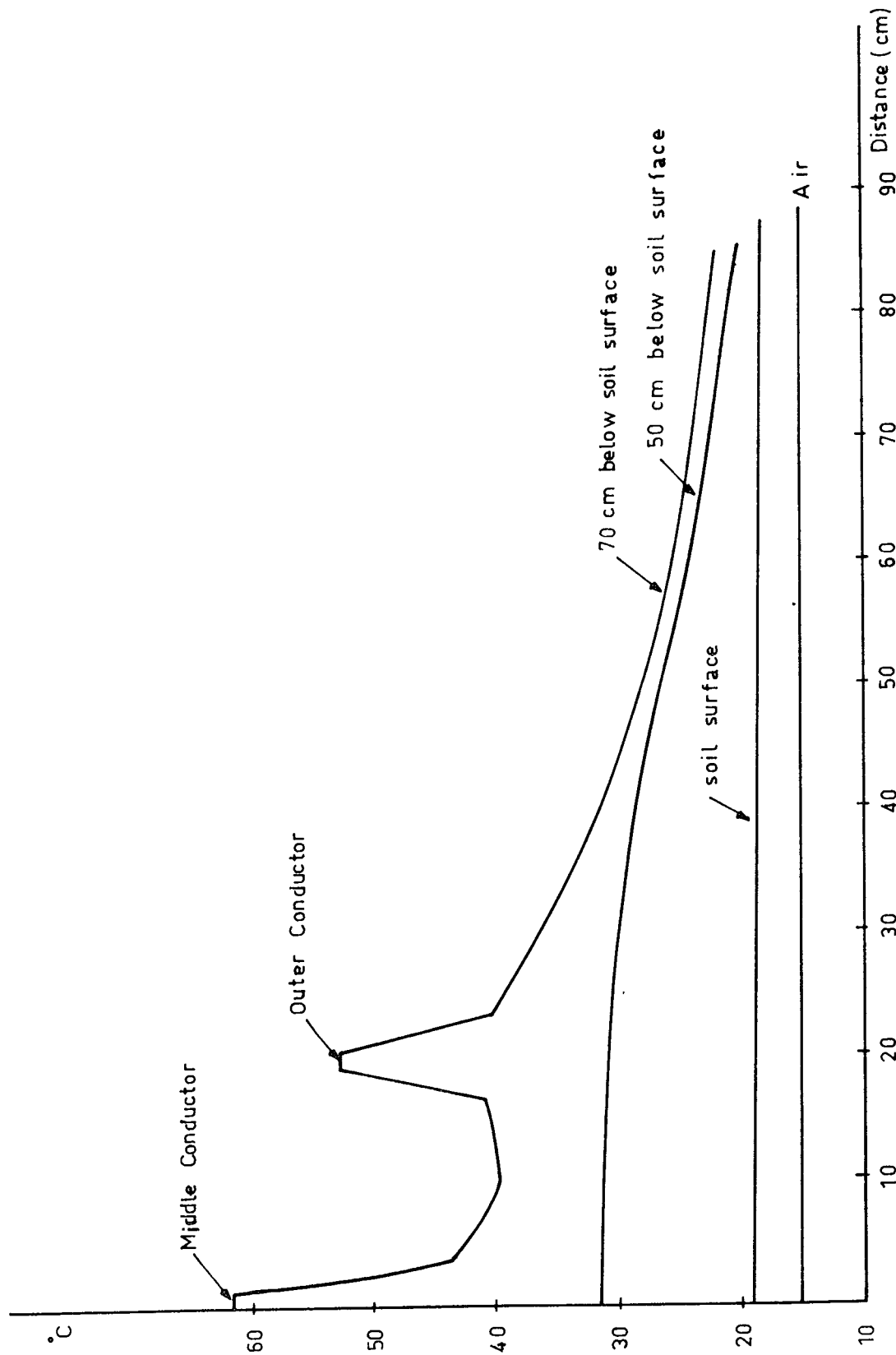


FIGURE 4.16 Temperature distribution at various parts of the region (at 120 minutes)

In Fig.4.16 the temperature variation as a function of distance from the symmetry plane at different depths below soil surface is plotted (at time  $t=120$  minutes)

A close examination of Fig.4.15 reveals that the highest temperature is obtained in the middle conductor. This is due to the fact that it is situated in the middle of both conductors and hence its heating is contributed also by these side conductors. Another reason is that the middle cable has comparatively higher shield losses (25 % of power loss). On the other hand the temperature variation of the middle shield and the soil 20 cm. above center of middle cable are very small. This is already expected due to the high thermal capacities of the insulation and the surrounding soil.

Fig.4.16 reveals that as we go away from the plane of symmetry the temperature at different depths below soil surface decreases to lower values finally tending to converge ambient temperature. The soil surface has a temperature which varies between 2 and 3°C above the air temperature. Since the value of the soil surface heat transfer coefficient is  $5 \text{ W/m}^2 \text{ } ^\circ\text{C}$ , thus 10-15  $\text{W/m}^2$  dissipates through the soil surface over the cables.

## CHAPTER V CONCLUSIONS

### 5.1 Concluding remarks on finite element approach

The advent of high speed digital computers and the development of numerical methods such as finite difference method and finite element method provides a great advantage in solving some engineering problems such as thermal transient problems for which analytical solutions can only be obtained for relatively simple geometries. In such methods, principle of superposition is applied for the fields due to heat sources and heat sinks, the soil thermal conductivity and thermal capacity are assumed to be constants, soil surface is assumed to be an isothermal (Kennelly hypothesis), radial symmetry for the cable model is to be considered (21). The electrical resistivity of the conductor is constant and equal to the value at steady state conductor temperature. The use of numerical methods such as finite element method with an efficient programming technique allows a progressive removal of some restrictions encountered in analytical methods.

One of the biggest headaches in applying the finite difference method occurs when either the arrangement of the nodes or the geometry is irregular. Finite element method simplifies many of these problems. Compared to the finite difference method the finite element method can more easily handle complicated boundary shapes and discontinuities in material properties. For example thermal analysis of a 3 phase cable can easily be achieved by finite element method, whereas the adoption of finite difference method is more difficult in that case. In the finite difference method the main concept is the approximation of derivatives by differences. In finite element method, however, approximation of integral derived in conjunction with the knowledge of calculus of variation.



Finite element solution approaches to the exact solution as the number of nodal points is increased, or in other words as the triangles with smaller dimensions are used, for which theoretical basis is introduced in the previous chapters.

In finite element formulation triangles are chosen as dividing the region into elements, since such elements are doing a much better job of approximating the circular regions (or boundaries).

Another important point in finite element formulation is the requirement for the computer storage. One of the biggest headache encountered in finite element method is the storage problem and this can easily be overcome by using the symmetrical and banded nature of the system matrices. For instance in three cables buried in soil there are 98 nodal points meaning that there will be 98 equations to solve. The nodal points have been numbered so that the maximum difference between the three node identifiers  $i$ ,  $j$  and  $k$  is 16. This means that there will be at most 16 diagonal lines above the main diagonal. Since the matrix is symmetrical, we will have to provide a storage for only  $17 \times 98 = 1666$  matrix components rather than  $98 \times 98 = 9604$  matrix components if the entire matrix was stored. The storage requirement for solving finite element equations is dominated by the coefficient matrix. The full matrix requires  $n^2$  coefficients to be stored, but this number is reduced to  $bn$  if the banded form described in previous chapters is used.

As with any numerical method employing a digital computer, a great deal of care must be taken to ensure that the program used has been thoroughly tested and that the data are supplied to it in the correct form. Especially the difficulty arises in the preparation of the finite mesh data.

Instead it is better to arrange finite element programs furnishing the mesh data automatically by itself. Although this might not be so easy for complicated geometries, when it is managed the computer would need to be given very limited number of data and in this way one possible source of error in data preparation will be overcome. Such an automatic mesh generation scheme is developed for semicircular regions in the single core simple cable problem.

Another advantage taken by the use of finite element method is obtained for calculating the thermal transients in buried three phase cable when the load current is a specified function of time, which of course would be a difficult job if any one of the analytical methods adopted.

## 5.2 Temperature transients in power cables

By the aid of a finite element program developed on the language fortran IV and run on Interdat 7/32 in the computer center of METU Gaziantep Campus, temperature transients in buried power cables are analysed. The analysis is made in two dimensions cartesian coordinates. First a simple cable problem for which steady state results are analytically available is analysed. It has been observed that at the end of 250 minutes, the transient results obtained by the developed program reach to almost steady state values. In equation solving both gaussian elimination and cholesky decomposition methods are tried and compared with each other. At the same time for both equation solving schemes rectangular array storage and full storage modes are utilised and the results are compared. It is seen that cholesky decomposition scheme employing the banded nature of the system matrices gives more efficient results in respect to the storage requirement and computer time.

A 35KV single phase Siemens Cable which is manufactured in

Turkey is analysed for different load currents and it is found that for load currents above 400A maximum permissible temperature of the polyethylene insulation ( $90^{\circ}\text{C}$ ) has been passed over. Another fact with this cable is that at this voltage level the main heat generation is due to the core losses. Dielectric losses at this voltage level has no significant role in heat generation.

Finally a 3 phase 275KV cable is analysed thermally under varying load conditions. At this voltage level heat generation due to the oil/paper insulation has a considerable effect on overall heating of the cable. In this case some amount of shield losses are introduced in the cable aluminium shield and its influence in the heating of the cable is included in addition to the power loss and dielectric losses.

### 5.3 Future work

The most important part of the finite element solution to a problem is the consideration for the storage requirement and computer time. Especially for very complicated geometries which results large number of algebraic equations to be solved present equation solving techniques might become ridiculous even if with highly developed digital computers. For most of the problems the system matrices are very sparse and even inside the band the zero coefficients very often far outnumber the non zero coefficients. Therefore more advanced techniques which takes advantage of this property should be developed and used especially for engineering problems of rather complex geometries.

APPENDIX A  
 VARIATIONAL FORMULATION

The use of a variational principle provides a powerful tool in formulating a finite element analysis. The general variational approach to the solution of a finite element problem is to seek a stationary value (often a minimum) for a quantity  $\chi$  which is defined by an appropriate integration of the unknowns over the solution domain. Such a quantity  $\chi$  is usually referred to as a 'functional'. When such a principle is used in a finite element analysis, the variation of  $\chi$  is carried out with respect to the values of the unknowns at the nodes of the mesh. To illustrate, necessary and sufficient conditions for the functional,

$$\chi = \iint \left\{ \frac{1}{2} k \left[ \left( \frac{\partial T}{\partial x} \right)^2 + \left( \frac{\partial T}{\partial y} \right)^2 \right] - (q - C \frac{\partial T}{\partial t}) T \right\} dx dy - \int_C Q T ds + \int_C \alpha \left( \frac{1}{2} T^2 - T_a T \right) ds \quad (A.1)$$

will be investigated, where last two integrals are taken along the boundary  $S$  enclosing the domain  $D$ , and where, the function  $T(x,y)$  is required to be continuous with piecewise continuous first derivatives in  $D+S$ . Fig. A.1 illustrates the solution domain with one part of the domain boundary.

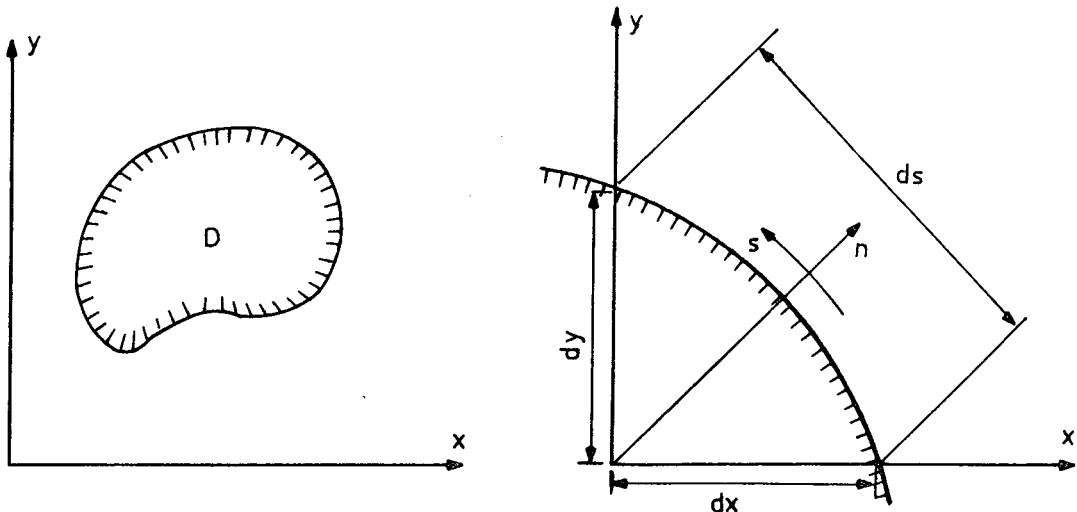


FIGURE A.1 A two dimensional solution domain with some part of the domain boundary.

The necessary condition for  $\chi$  to be stationary is that the variation of  $\chi$ ,  $\delta\chi$ , vanishes;

$$\begin{aligned} \delta\chi = & \int_D k \left[ \frac{\partial T}{\partial x} \delta\left(\frac{\partial T}{\partial x}\right) + \frac{\partial T}{\partial y} \delta\left(\frac{\partial T}{\partial y}\right) \right] dD - \int_D (q - c \frac{\partial T}{\partial t}) \delta T dD \\ & - \int_S q \delta T dS + \int_S \alpha (T - T_a) \delta T dS \end{aligned} \quad (A.2)$$

Noting that

$$\delta \left( \frac{\partial T}{\partial x} \right) = \frac{\partial}{\partial x} (\delta T),$$

$$\delta \left( \frac{\partial T}{\partial y} \right) = \frac{\partial}{\partial y} (\delta T).$$

allows eq.(A.2) to be written as

$$\begin{aligned} \delta\chi = & \int_D k \left[ \frac{\partial T}{\partial x} \frac{\partial}{\partial x} (\delta T) + \frac{\partial T}{\partial y} \frac{\partial}{\partial y} (\delta T) \right] dD - \int_D (q - c \frac{\partial T}{\partial t}) \delta T dD \\ & - \int_S q \delta T dS + \int_S \alpha (T - T_a) \delta T dS \end{aligned} \quad (A.3)$$

Green's theorem can be written in the form;

$$\begin{aligned} \int_D \left( \frac{\partial u}{\partial x} \frac{\partial v}{\partial x} + \frac{\partial u}{\partial y} \frac{\partial v}{\partial y} \right) dD = & - \int_D v \left( \frac{\partial^2 u}{\partial x^2} + \frac{\partial^2 u}{\partial y^2} \right) dD \\ & + \int_S v \left( \frac{\partial u}{\partial x} n_x + \frac{\partial u}{\partial y} n_y \right) dS \end{aligned} \quad (A.4)$$

where  $n_x$ ,  $n_y$  are the x, y components of the unit outward normal to S, denoted by n. The functions  $u = u(x, y)$  and  $v = v(x, y)$  are required to be continuous in D+S. The first and second derivatives of the same functions are required to be piecewise continuous(10).

Considering the T and  $\delta T$  and their first derivatives are continuous green's identity(A.4) can be applied into(A.3) as follows.

$$\begin{aligned} \delta\chi = & - \int_D k \nabla^2 T \delta T dD - \int_D (q - c \frac{\partial T}{\partial t}) \delta T dD + \int_S \frac{\partial T}{\partial n} \delta T dS \\ & - \int_S q \delta T dS + \int_S \alpha (T - T_a) \delta T dS \end{aligned} \quad (A.5)$$

where

$$\nabla^2 T = \frac{\partial^2 T}{\partial x^2} + \frac{\partial^2 T}{\partial y^2}$$

and

$$\frac{\partial T}{\partial n} = \frac{\partial T}{\partial x} n_x + \frac{\partial T}{\partial y} n_y$$

Since the domain and surface integral in eq.(A.5) are independent, it follows that

$$-\int_D \left[ k \nabla^2 T - (q - c \frac{\partial T}{\partial t}) \right] \delta T dD = 0 \quad (A.6)$$

and

$$\int_S \left( k \frac{\partial T}{\partial n} + \alpha(T - T_a) - Q \right) \delta T dS = 0 \quad (A.7)$$

from the arbitrariness of  $\delta T$  in  $D$ , it follows that equation (A.6) and (A.7) takes the following forms,

$$k \nabla^2 T + q = c \frac{\partial T}{\partial t} \quad \text{in } D \quad (A.8)$$

$$\frac{\partial T}{\partial n} + \frac{\alpha}{k}(T - T_a) - \frac{Q}{k} = 0 \quad \text{on } S \quad (A.9)$$

Eq.(A.8) is the governing parabolic differential equation for a transient heat conduction problem.  $\alpha(T - T_a)$  and  $Q$  in eq.(A.9) are the boundary conditions specified on the boundary of the solution domain.

Alternatively if  $T(x,y)$  is prescribed as  $T=g$  on that part of the boundary denoted  $S_1$ , so that,

$$T=g \quad \text{on } S_1$$

and not on the remaining part, denoted  $S_2$  where,

$$S=S_1+S_2$$

Then the variations of  $T$  must vanish on  $S_1$ ; that is

$$\delta T = 0 \quad \text{on } S_1$$

This time eq.(A.9) being valid on  $S_2$

Therefore in order to solve a second order partial differential equation representing any physical problem (in this case, transient heat conduction) with specified boundary conditions, one must find a trial function  $T(x,y)$  which, when substituted, makes the integral equation (A.1) stationary, and this function will provide the solution.

For many physical problems, variational principles have been developed giving rise to a functional whose stationary conditions yield the solution to the problem. But for problems in which exact variational forms can not be found, the Galerkin method or a similar residual method can be utilized to arrive at the integral equations of the specific problem.

APPENDIX B  
HIGHER ORDER SHAPE FUNCTIONS DERIVED  
FROM AREA COORDINATES

With the help of area coordinates, it is possible to construct shape functions for different kinds of elements. Table(B.1) gives a listing of such functions for linear, quadratic and cubic triangular elements.

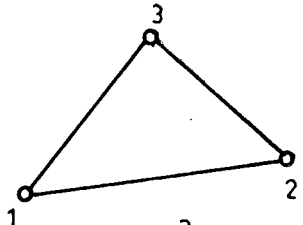
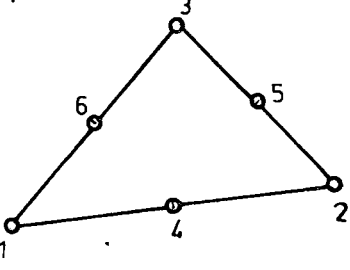
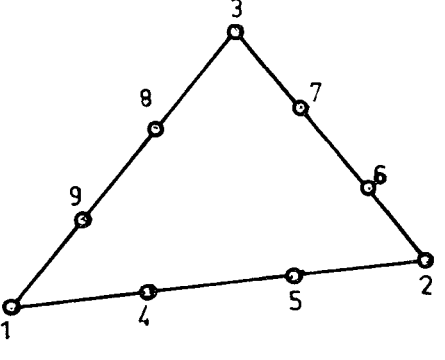
Family of triangular elements	Shape functions in terms of area coordinates
<p>Linear</p> 	$N_1 = w_1$ $N_2 = w_2$ $N_3 = w_3$ <p>Corner nodes</p>
<p>Quadratic</p> 	$N_1 = (2w_1 - 1)w_1$ $N_2 = (2w_2 - 1)w_2$ $N_3 = (2w_3 - 1)w_3$ <p>Midside nodes</p> $N_4 = 4w_1 w_2$ $N_5 = 4w_2 w_3$ $N_6 = 4w_3 w_1$ <p>Corner nodes</p>
<p>Cubic</p> 	$N_1 = \frac{1}{2} (3w_1 - 1) (3w_1 - 2)w_1$ $N_2 = \frac{1}{2} (3w_2 - 1) (3w_2 - 2)w_2$ $N_3 = \frac{1}{2} (3w_3 - 1) (3w_3 - 2)w_3$ <p>Edge nodes</p> $N_4 = \frac{9}{2} w_1 w_2 (3w_1 - 1)$ $N_5 = \frac{9}{2} w_1 w_2 (3w_2 - 1)$ $N_6 = \frac{9}{2} w_2 w_3 (3w_2 - 1)$ $N_7 = \frac{9}{2} w_2 w_3 (3w_3 - 1)$ $N_8 = \frac{9}{2} w_3 w_1 (3w_3 - 1)$ $N_9 = \frac{9}{2} w_3 w_1 (3w_1 - 1)$ <p>Internal node</p> $N_{10} = 27w_1 w_2 w_3$

TABLE.B.1 Higher order shape functions



APPENDIX C  
 EXACT SOLUTION OF STEADY STATE TEMPERATURE  
 DISTRIBUTION IN INSULATED ELECTRIC CABLE

Assume a cross section of an electric cable as shown in Fig.C.1. The temperature change is designated by  $dT$ . Then the differential rate of heat flow for  $L=1$ (one unit of length of cable) through the cylindrical concentric surfaces may be written(22),

$$dq = - kA (dT/dr) = -kr d\phi(1)(dT/dr) \quad (C.1)$$

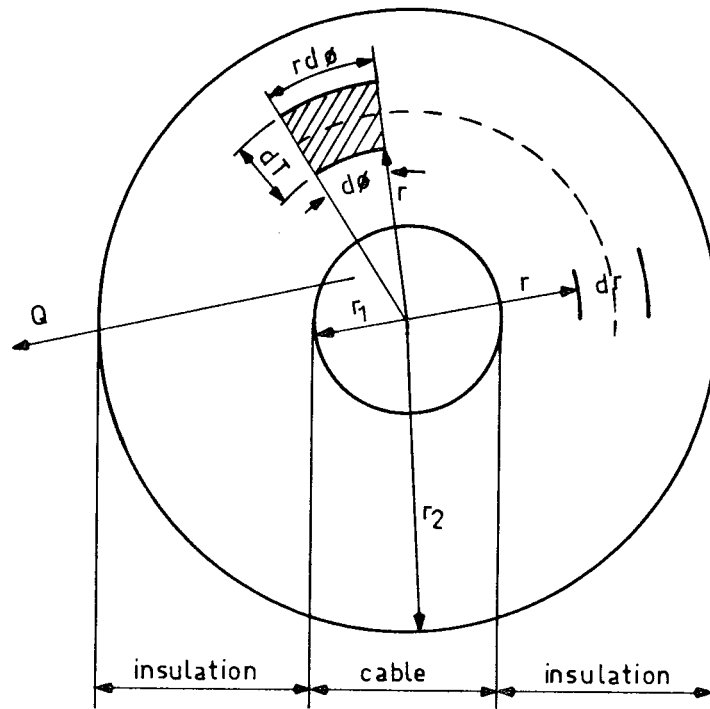


FIGURE C.1 Cross section of an insulated power cable.

The minus sign meaning that with increase of  $r$  the temperature decreases ( direction of heat flow is from the warmer region in the core of cable to cooler one).

Integrating equation(C.1) first with respect to  $\varnothing$  from  $\varnothing=0$  to  $\varnothing=2\pi$ , obtain

$$\frac{1}{k} \frac{dr}{r} \int_0^q dq = - dT \int_0^{2\pi} d\varnothing ,$$

$$q \frac{dr}{r} = - 2\pi k dT \quad (C.2)$$

then integrate eq.(C.2) with respect to  $r$  from  $r$  to  $r_2=b$  and  $T$  from  $T(r)$  to  $T(b)$

$$q \int_r^b \frac{dr}{r} = -2\pi k \int_{T(r)}^{T(b)} dT$$

$$q \ln(b/r) = 2\pi k ( T(r)-T(b) )$$

calling  $f_c = \frac{q}{2\pi a}$  is the heat flux generated by cable core

$$T(r) = T(b) + \frac{a}{k} f_c (\ln b/r)$$

gives the temperature at any radial position  $r$ .

## REFERENCES

- 1 . M.J.Turner, R.W.clough, H.C.Martin, and L.J Topp, stiffness and deflection analysis of complex structures, J.Aeronaut.Sci.23, No.9, 805-824, September 1951.
- 2 . O.C. Zienkiewicz, " The finite element method in engineering science ", Mc Graw.Hill, 1971.
- 3 . Çetin E., " Field analysis by the method of finite elements ", M.Sc.Thesis, METU, 1978.
- 4 . J.P.Holman., " Heat transfer ", Mc Graw-Hill Kogakusha Ltd, 1976
- 5 . Hippel A, " Dielectric materials ", Wiley, New York, 1954
- 6 . J.C. Anderson, " Dielectrics ", London, Chapman and Hall, 1964.
- 7 . Y K Cheung and M F Yeo, " A practical introduction to finite element analysis ", Pitman, 1979
- 8 . Glen E. Myers, " Analytical methods in conduction heat transfer ", Mc Graw-Hill, 1971
- 9 . Aral M., " Finite element solutions of selected partial differential equations ", METU, 1974.
10. D.H Norrie, " Finite element methods, fundamentals and applications, ", New York Academic Press, 1973
11. V.N.Faddeeva, " Computational methods of linear algebra ", Dover publications, 1956

12. World Energy Congress X, İstanbul,
13. 3. Genel Enerji Kongresi Tebliğleri.
14. M. Rehowicz, " Electric power at low temperatures ", clarendon Press. Oxford, 1975
15. H.S. Carslaw and J.C. Jaeger, " Conduction of heat in solids ", Oxford, Clarendon Press, 1959
16. Croft and Lilley, " Heat transfer calculations using finite difference equations ", applied science publishers Ltd, London, 1977
17. Bağcıoğlu T., " Transient field analysis of underground cables ", M.Sc. Thesis, METU, 1978
18. Siemens, Protothen-x Kablolar broşürü, 1979.
19. Akar M., " Numerical solution of transient-state thermal field distributions of underground cables ", M.Sc.Thesis, METU, 1981.
20. N.Flatabo, " Transient heat conduction problems in power cables solved by finite element method ", IEEE transactions on PAS-92, Jan/Feb 1973, pp.56-63
21. Dommelen, Van den Broeck, Steffens, " Two dimensional quasi stationary temperature rise in multicable configurations under arbitrary cyclic load, " IEEE transactions on PAS-98, No.1 Jan/Feb 1979
22. Alfreds R. Jumikis, " Thermal soil mechanics ", Rutgers university press, 1966.